GEOLOGICAL SURVEY OF ESTONIA

Geological background and seismicity of the prospective wind farm area offshore Sõrve peninsula, western Saaremaa

RAKVERE 2025

Cover photo: Collage.

Recommended citation style: Tuuling, I., Suuroja, S., Veski, A., Soosalu, H., Karpin, V. 2025. Geological background and seismicity of the prospective wind farm area offshore Sõrve peninsula, western Saaremaa. Geological Survey of Estonia, Rakvere.

AFFIRMED
Geological Survey of Estonia
Decision of research council

Geological background and seismicity of the prospective wind farm area offshore Sõrve peninsula, western Saaremaa

RESEARCH REPORT

Authors: Igor Tuuling, Sten Suuroja, Anu Veski, Heidi Soosalu, Vladimir Karpin

Leader of working group: Sten Suuroja

Director of the Geological Survey of Estonia: Sirli Sipp Kulli

RAKVERE 2025

Contents

List of Tables

List of Figures

Abstract

This report deals with the geological background and seismicity of a potential wind farm area (WFA), a 7-shaped polygon framed offshore western Saaremaa, some 10–40 km off the Sõrve peninsula. No particular geological/geophysical research was carried out for this report. All the descriptions and conclusions about the geological background presented rely on interpretations of two former seismo-acoustic/multibeam data sets available from this area: 1) The Swedish-Estonian airgun (250–500 Hz) study on the bedrock strata of the central Baltic Sea from early 1990s and, 2) the seafloor mapping data set collected in 2017–2024 by the Estonian Maritime Administration using a multibeam sonar and chirp-type (2–9 kHz) seismo-acoustic transmitter.

Sea depth offshore the Sõrve peninsula increases in the east-west direction towards the central Baltic Sea. The depth varies within the wind farm polygon from 12 to 45 m around its SE and NW corners, respectively. In general, two separate sea depth areas with different geological settings emerge around the WFA. Shallow marine areas (approximately up to -30 m), which emerge intermittently along the margins of the 7-shaped wind farm polygon, represent higher patches of the limestone plateau surrounding the WFA from the east and the north. The deeper sea area (roughly, deeper than 30–35 m) is found above the bedrock slope-depression area in the form of solitary deep valleys that have been carved into the clayey, easily erodible limestones of the Kuressaare, Kaugatuma and Ohessaare stages. The depth of the bedrock varies largely between 25–30 m and 40–60 m below sea level within the limestone plateau and slope-depression portions of the WFA, respectively. However, the depth of the bedrock may possibly exceed 80 m b.s.l. in the valleys incised into the limestone slope.

Available seismo-acoustic data from a chirp-type transmitter do not enable to separate the layer of glacial till, and thus to distinguish unambiguously between the seismo-acoustically impenetrable glacial till and bedrock surfaces. Based on some airgun and chirp-type seismo-acoustic data, however, glacial till sediments occur at least sporadically around the WFA. The postglacial Quaternary sequence around the WFA reveals two widespread units when penetrated by the seismo-acoustic pulse. The seismic signature of the unit that rests on the impenetrable glacial till/bedrock surface reminds waterlain glacial diamicton, i.e. a clay-rich layer containing abundantly small rock pieces and pebbles. Upwards the section, the latter unit is overlain by a layer of the Baltic Ice Lake varved clays. The waterlain glacial diamicton is found widely all over the WFA and makes up a substantial part of the sediments that are exposed within the shallow-marine areas across the limestone plateau. Still, it may be occasionally absent within the outcropping bedrock patches. The thickness of this unit may vary from virtually zero to up to 10 m in the bedrock depression and valleys. The varved clay unit was deposited, and is thus exposed only within the low-lying bedrock slope-depression area, where its thickness varies largely between 3–6 m. However, the thickness may slightly exceed 10 m in bedrock valleys. To distinguish and follow the glacial till surface unambiguously, an additional study is needed where chirp- and boomer-type transmitters are operated simultaneously.

The sea bottom around the bedrock slope-depression area of the WFA is covered widely with loose, easily movable sandy sediments. Numerous smaller and large boulders emerge on the seafloor above the outcropping limestone plateau patches covered with the thin layer of the glacial till or waterlain glacial diamicton that arise along the nearshore eastern boundary of the 7-shaped wind farm polygon.

The region of Estonia is geologically stable and only modestly seismically active. Sporadic occurrence of minor (magnitude < 3) earthquakes is typical. It is a challenge to form a comprehensive understanding of seismicity in such an area of low activity. Data spanning centuries would be needed, but historical data are patchy and somewhat inaccurate. Instrumental observations providing quite reliable locations and other earthquake parameters exist only for recent decades. For earlier times only macroseismic observations exist, i.e., earthquake sizes and locations are estimated basing on the impact on people, buildings and landscape.

A few small earthquakes, both historical and instrumentally recorded, have been noted in the surroundings of the WFA. The data are too sparse for drawing definite conclusions on seismicity of the region. However, it can be stated that the level of seismicity, and further on seismic hazard, is modest.

1. Geological background of the WFA off the Sõrve peninsula

1.1. Introduction

Globally escalating energy crisis with skyrocketing electricity costs has drastically increased demand for green and sustainable energy sources. Wind is considered one of Estonia's most prospective energy sources due to the extensive Baltic Sea coastline with large shallow offshore areas. These circumstances have initiated several wind farm (WF) projects that have been realised mostly in nearshore regions on mainland during the last couple of decades. However, as experience in other countries has shown, offshore areas have much higher and stable wind potential, disturb less people's everyday life, and might therefore be even better choice for erecting WFs. To pick up a suitable site for any construction offshore is a complex process that, besides evaluating environmental, navigational, fishing etc. hazards/complications, expects undoubtedly a good knowledge of the sub-bottom geology of the area. Geological structure (the age and type of the rocks, thicknesses of the formed sediments and rocks, presence and intensity of faulting etc.) of any area is dependent on its global plate tectonic setting throughout the geological history. This determines also probability for the present tectonic and seismic activities and hazard of possible earthquakes in Estonia.

Regular marine geological studies in Estonia commenced in 1973, when a marine geological research group was introduced at the Institute of Geology of the Estonian Academy of Sciences. Since then, a large amount of different kinds of geological information has been collected from the shallow marine areas offshore Estonia. Nowadays, marine geological studies are primarily based on different kinds of seismo-acoustic methods. These methods have been growingly and more efficiently applied in Estonia since the late 1980s. Besides geological studies, Estonian Maritime Administration commenced a seafloor mapping of the Estonian territorial waters in early 1990s, using different sonar-based techniques (side scan- and multibeam-sonar, seismo-acoustic profiling with a chirp-type sound transmitter). Thus, a substantial seismo-acoustic database with varying quality has been assembled from the Estonian offshore areas for a period of more than 40 years.

ELWIND is a joint Estonian-Latvian state-run cross-border offshore wind project in the Baltic Sea (https://elwindoffshore.eu/elwind/#elwind-et). Project developer is Environmental Investment Centre. Project partners are Ministry of Climate from Estonia and Ministry of Economics from Latvia. According to the official development strategy, the shallow-marine area west of the Saaremaa Island is considered as one of the prospective regions for erecting WFs offshore Estonia. Based on all available data collected on- and offshore areas around western Saaremaa, the aim of the present report is to summarize the geological background of the wind farm area (WFA) outlined some 10–40 km to the west-southwest of the Sõrve peninsula (Fig. 1). As the shape of the area reminds a 7-shaped (resembling number seven) polygon, two transversely oriented sections can be distinguished in the WFA. An about 3–8 km wide and 20 km long E-W section extending towards the central Baltic Sea in the north intersects with an about 1–5 km wide and 30 km long NE-SW trending nearshore segment that follows largely the shoreline of the Sõrve peninsula.

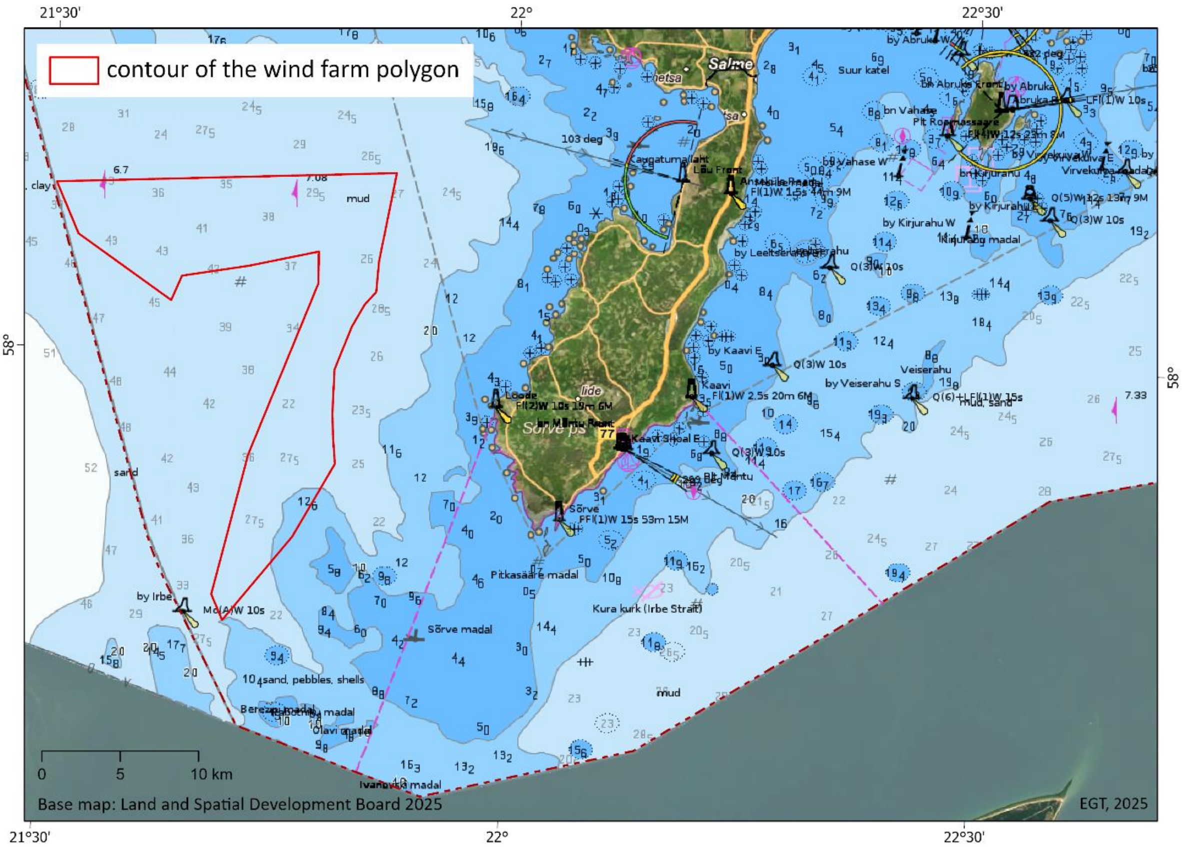

Fig. 1. Location of the 7-shaped wind farm polygon outlined offshore WSW of the Sõrve peninsula on the maritime chart of Estonia

1.2. Used geological materials/data

The construction basement for wind turbines, the uppermost section of the subsurface sediments/rocks in Estonia can be lithologically divided roughly into two portions with contrasting geotechnical parameters. Unconsolidated soft sediment package of the Quaternary cover with varying thickness and composition overlays the solid and hard Palaeozoic bedrock sequence. The bedrock exposed on Saaremaa, as well as in the offshore areas around the island is made up of Silurian limestones with highly varying clay content and resistant to the erosion.

There are lot of data published on the geology of the Estonian island of Saaremaa. Most of our knowledge is based on geological mapping or specific scientific studies that have been carried out by the Geological Survey of Estonia or by the Institute of Geology of the Estonian Academy of Sciences, respectively, during the second half of the XX century. Besides many scientific papers, there are two monographs dealing with the Silurian bedrock around Saaremaa (Kaljo, 1970, 1977), as the data on the Quaternary sequence are scattered across numerous publications/monographs (e.g. Raukas, 1978; Tavast & Raukas, 1982). All this information is furthermore summarized in a monograph dealing with the geology and mineral resources of Estonia (Raukas & Teedumäe, 1997).

Although preliminary marine geological studies in Estonia were carried out already in 1970–1980s (Lutt & Raukas, 1993), systematic seismo-acoustic profiling with gradually improving equipment and quality of recordings started only when a Swedish-Estonian cooperation project was initiated in early 1990s. As this project was concentrating largely on the bedrock geology, an analogue single channel equipment with a low frequency seismic transmitter (A PAR-600 air gun at 12 MP) at frequency range 250–500 Hz was mainly used to get deeper penetration of the seismic pulse into the solid limestone sequence. Several seismic profiles shot during that project cover also the WFA west of the Sõrve peninsula (Fig. 1; see also Fig. 12). The results of this project are published in numerous papers, many of which describe the geological background of the Silurian stratal sequence around the WFA and its correlation with the nearby drill core sections on the Island of Saaremaa (Tuuling & Flodén, 2009, 2011, 2013). Thus, the bedrock data and conclusions concerning the WFA offshore western Saaremaa are largely based on the results achieved during the Swedish-Estonian scientific project.

Compared to the relatively well-studied Silurian strata, the Quaternary sequence around the WFA is poorly explored. This is foremost because the sound transmitter (airgun) used during the Swedish-Estonian project did not give sufficient resolution for subdividing and studying the Quaternary layers more in detail. However, seafloor mapping of the Estonian nearshore areas performed in the recent years by the Estonian Maritime Administration has produced plenty of high-resolution seismo-acoustic (chirp-type transmitter and multibeam sonar) data on the uppermost, i.e. the postglacial Baltic Sea section of the Quaternary sequence off the Sõrve peninsula. Thus, the overview of the postglacial Quaternary sequence around the WFA presented in this report relies substantially on seismo-acoustic data generated by the chirp-type transmitter. The multibeam sonar, however, provides us with valuable information about the details of the seafloor relief, as well as about the hardness of the substrate (possible types of the rocks and sediments) exposed on the seafloor.

1.3. Seafloor morphology and substrate

A set of bathymetry and backscatter maps were composed for the WFA based on the chirp-type seismo-acoustic and multibeam sonar data (see the net of the chirp and multibeam sonar profiles in Fig. 21) collected by the Estonian Maritime Administration (Figs 2–8, 8A).

Bathymetric data were collected during routine hydrographic surveys by the Estonian Transport Administration from 2017 to 2024 onboard the research vessel *Jakob Prei* using a Reson 7125 and Reson T50 MBES operating at 400 kHz and utilizing 256 to 512 equiangular beams, with a swath width varying from 130° to 140°. The vessel's speed was maintained at 12 knots and the overlap between the neighboring swathes was around 10%.

Bathymetric data was recorded and processed using in-house software RAN/AEGIR. The data collected by RAN/AEGIR is in a proprietary format. The processed data was exported in a XYZ format and gridded as a 2.5 m average grid using Qimera 2 software.

The backscatter data were collected in parallel with bathymetric data. Meridata MDPS software was used to process backscatter data and generate average grids at 2.5 m resolution.

As already shown on the maritime chart (Fig. 1), sea depth off the Sõrve peninsula has a regular increasing trend from E to W towards the central Baltic Sea. The same tendency, the sea deepening to the WSW emerges also on the bathymetry maps within the 7-shaped wind farm polygon, where the sea depth varies from about 12 m to nearly up to 45 m around its south-eastern and north-western corners, respectively (Figs 2–7). Thus, along the 3–8 km wide and 20 km long E-W trending northern section of the wind farm polygon, sea depth increases from about 27–28 up to 45 m (Fig. 4). Sea depth remains largely in the limits of 25–35 m within the 1–5 km wide and 30 km long NE-SW trending shoreward section of the wind farm polygon (Fig. 4). Exceptionally, a cape-like elevation, likely of bedrock origin, intrudes into the southern part of the latter section, where the seafloor rises to -12 m (Figs 2–7)

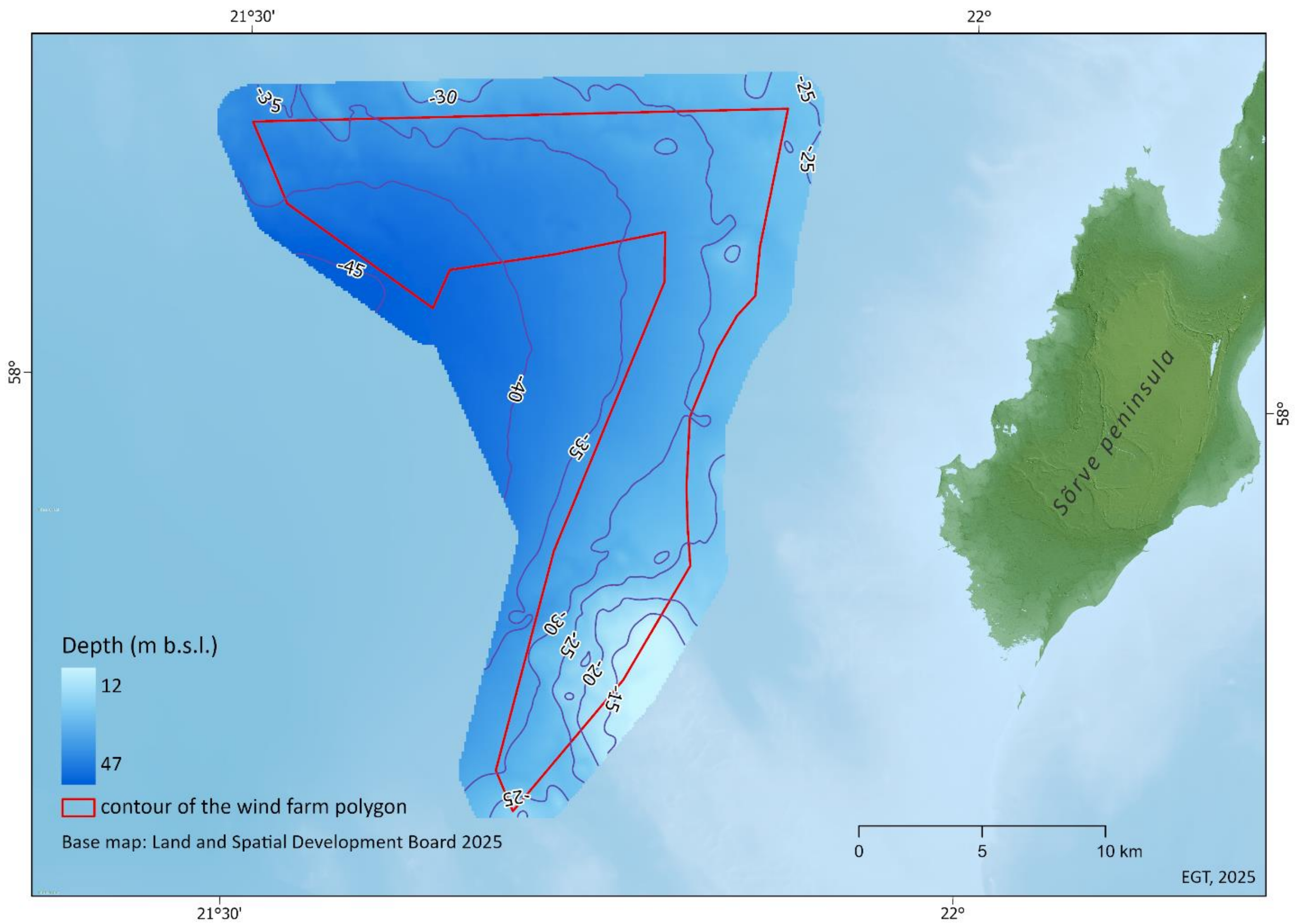

Fig. 2. Bathymetry map of the WFA based on chirp-generated seismo-acoustic data

Considering the smoothness of the sea bottom, the 7-shaped wind farm polygon surrounding the WSW deepening seafloor depression from E and N (Fig. 2) reveals two visibly separate areas. The boundary between the levelled and rugged seafloors coincides largely with the -30 and -35 m depth isolines running within the NE-SW and E-W trending segments of the 7-shaped wind farm polygon, respectively (Fig. 2). Similar smoothness difference is obviously due to the background (elevation) of the bedrock relief and the type of the sediments/rocks exposed on the sea bottom. In the areas deeper than 30–35 m, the bedrock depression becomes infilled, and thus the seafloor levelled by the postglacial soft clayey Baltic Sea sediments. According to the chirp-type seismo-acoustic data (discussed further in the Quaternary chapter), these sediments are represented by layers of the Baltic Ice Lake varved clays and waterlain glacial diamicton. The proportion of Baltic Sea clayey sediments is insignificant or possibly non-existent outside the bedrock depression, i.e. in the areas with higher bedrock surface to the north and east of the -35 and -30 m depth isolines, respectively. Thus, glacial till or even the Silurian bedrock may occasionally crop out along the margins of the WFA north and east of the -35 and -30 m depth isolines, respectively. Patches with more solid (hard) seafloor substrate on the multibeam backscatter and echo sounder maps (Figs 8, 8A) support the latter argument.

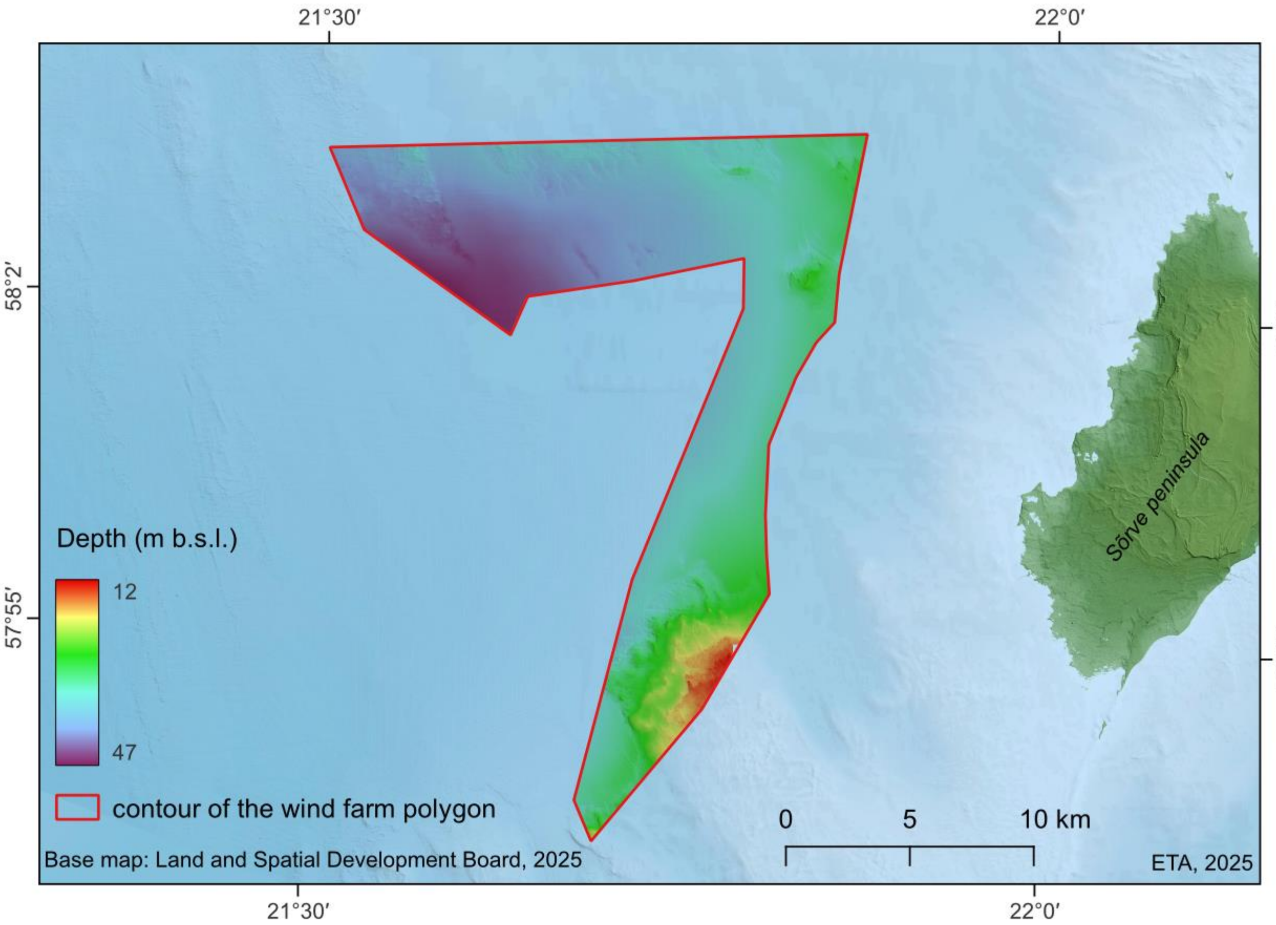

Fig. 3. Bathymetry map of the WFA based on multibeam echo-sounding data

The rugged bottom relief is best demonstrated around the southern corner of the NE-SW trending segment of the wind farm polygon, where aforementioned cape-like bedrock elevation reaching 12 m b.s.l. intrudes into the WFA (Figs 3-7). Another area with visibly rugged bottom relief emerges around the NE corner and along the north margin of the WFA, where multibeam backscatter data reveal numerous hard substrate outcrops, obviously limestone or glacial till patches overlain with a thin layer of postglacial clayey sediments (as discussed in the Quaternary chapter, likely by the waterlain glacial diamicton) (Figs 6-8, 8A). A significant number of boulders with varying size occur around these shallow-marine bedrock/glacial till and waterlain glacial diamicton outcrops with rugged bottom relief (Figs 6, 7). Scour marks of relict icebergs and large ripple marks possibly caused by bottom currents emerge at the transition from the rugged relief area to the levelled seafloor. The ripple marks (Fig. 6; see also Figs 22, 28) prove that the sea bottom is widely covered by a thin layer of loose and easily movable sandy sediments in the deeper areas of the WFA, where the postglacial Baltic Ice Lake varved clays are largely exposed. Similar bottom structures are very common and well-studied in this region (Karpin et al., 2021).

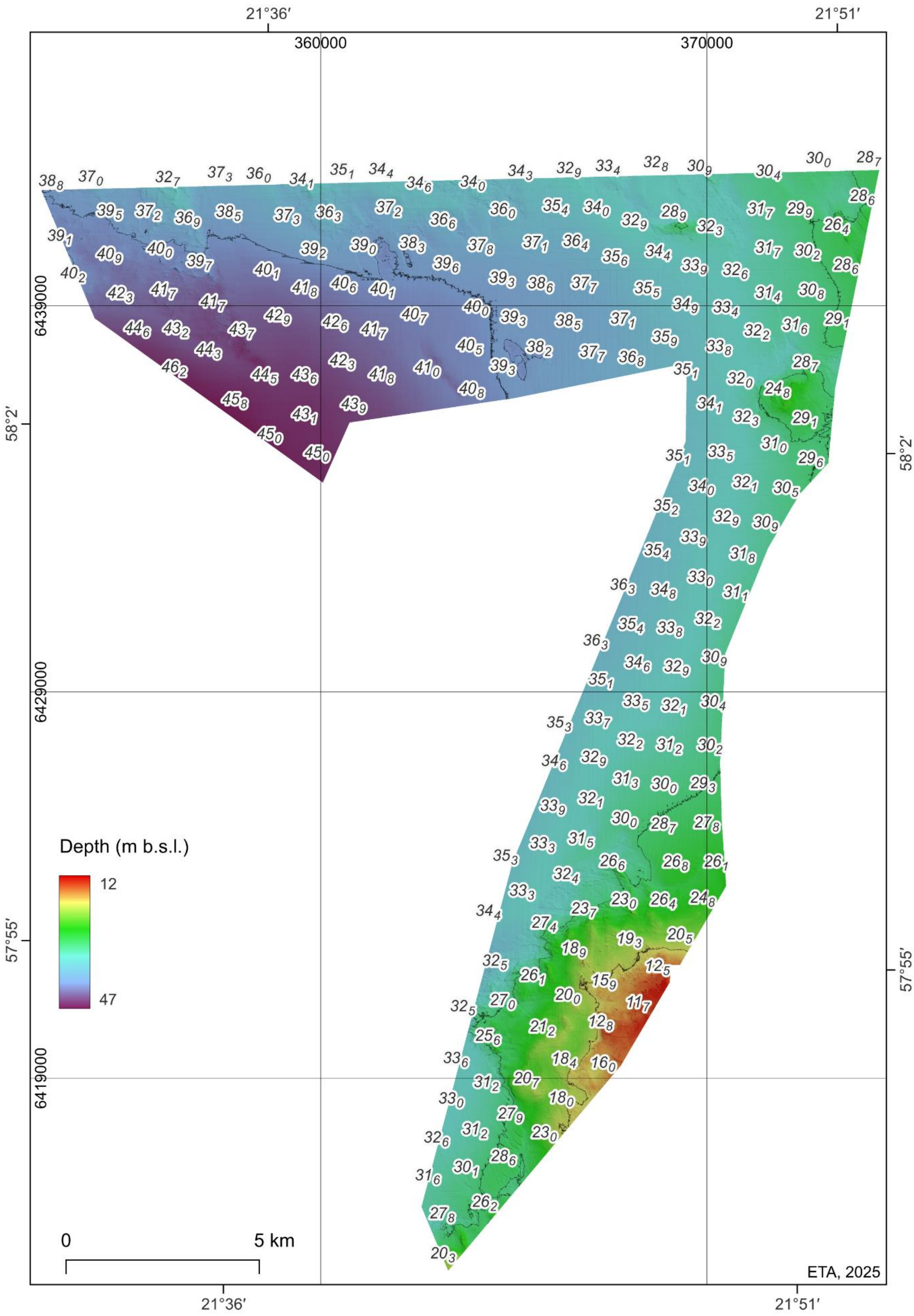

Fig. 4. Enlarged multibeam echo-sounding bathymetry map of the WFA with the sea depth values

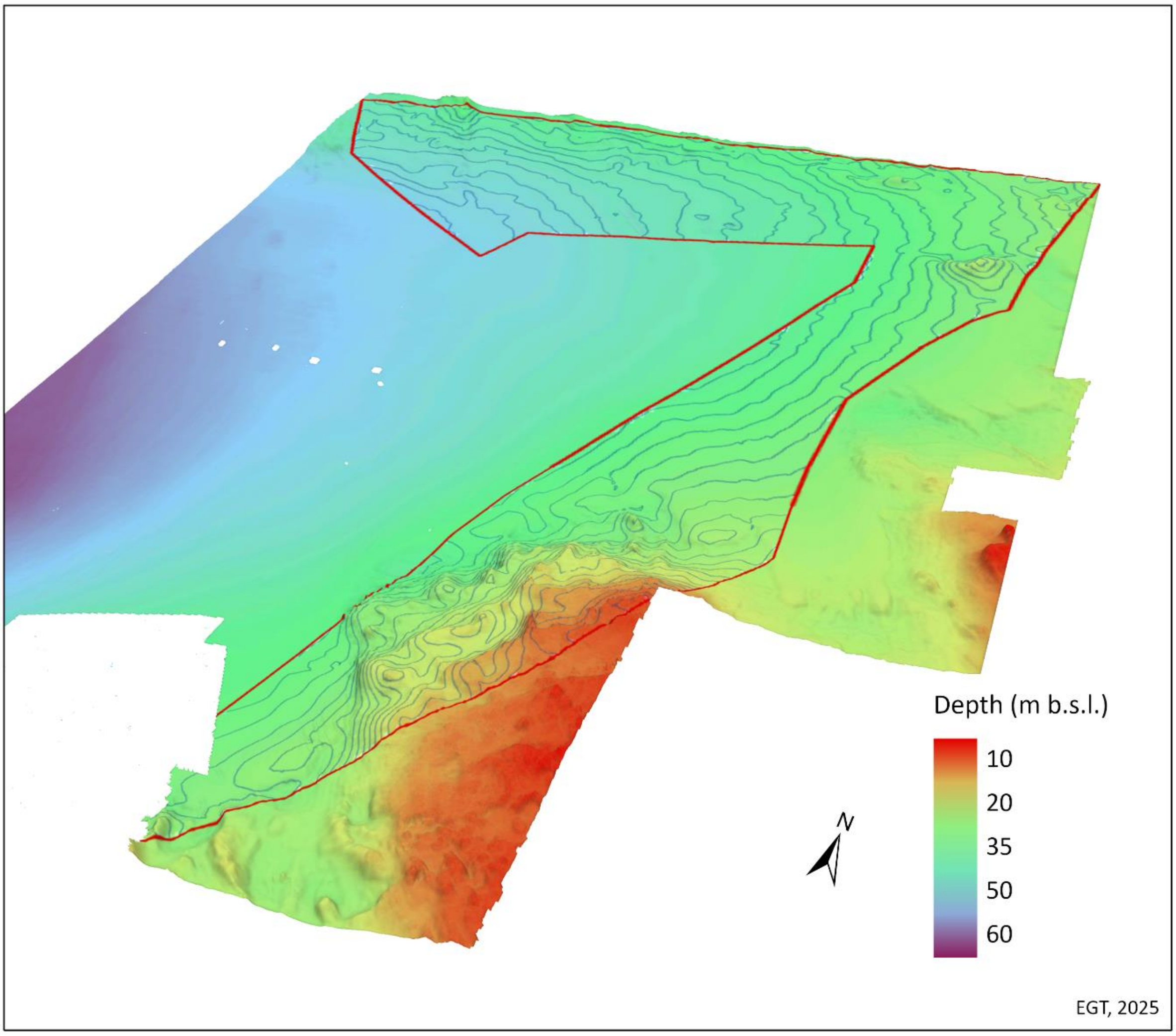

Fig. 5. 3D view of the seafloor relief around the WFA based on multibeam echo-sounding data

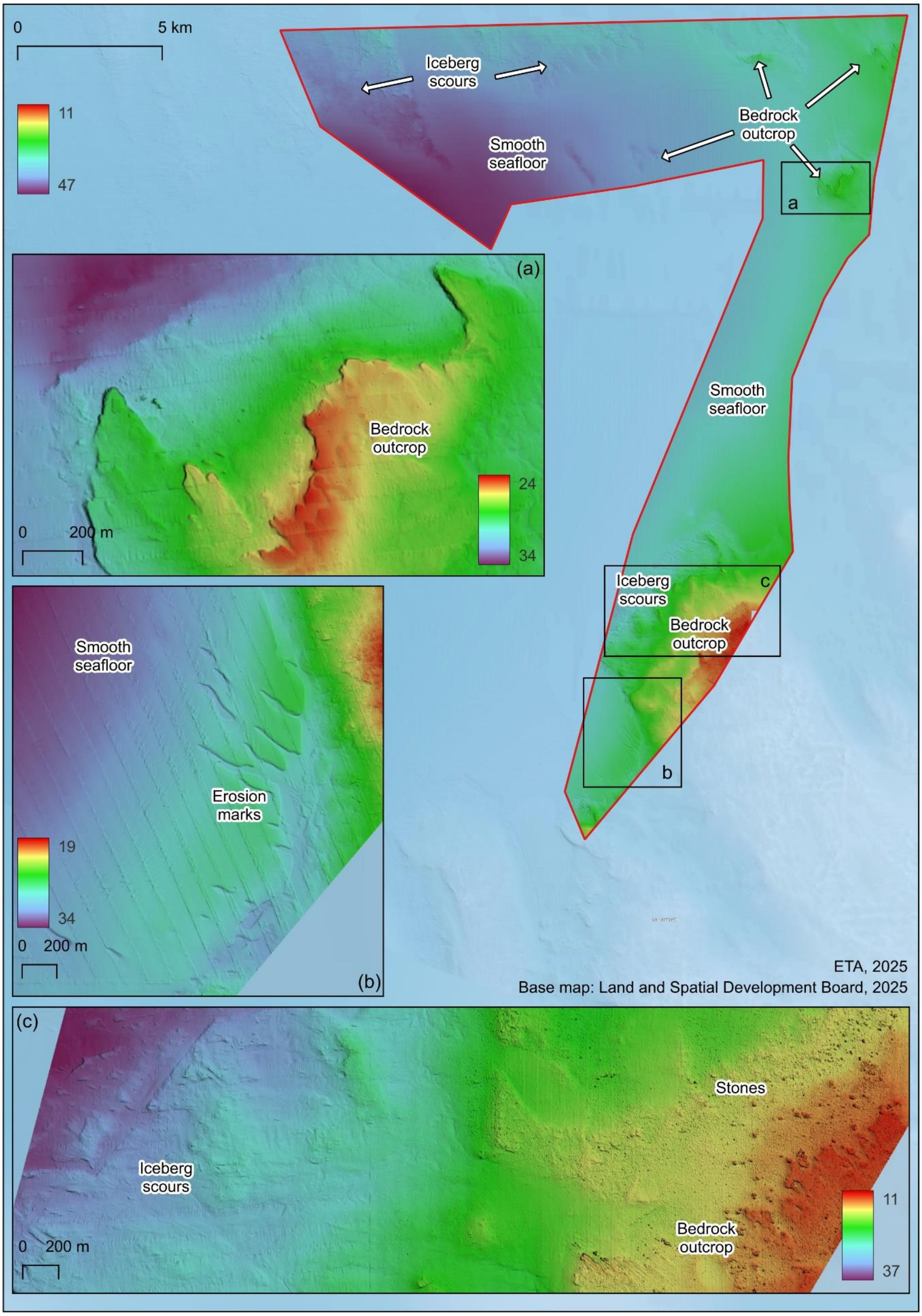

Fig. 6. Geomorphological features on the seafloor of the WFA with enlarged excerpts based on multibeam echo-sounding data

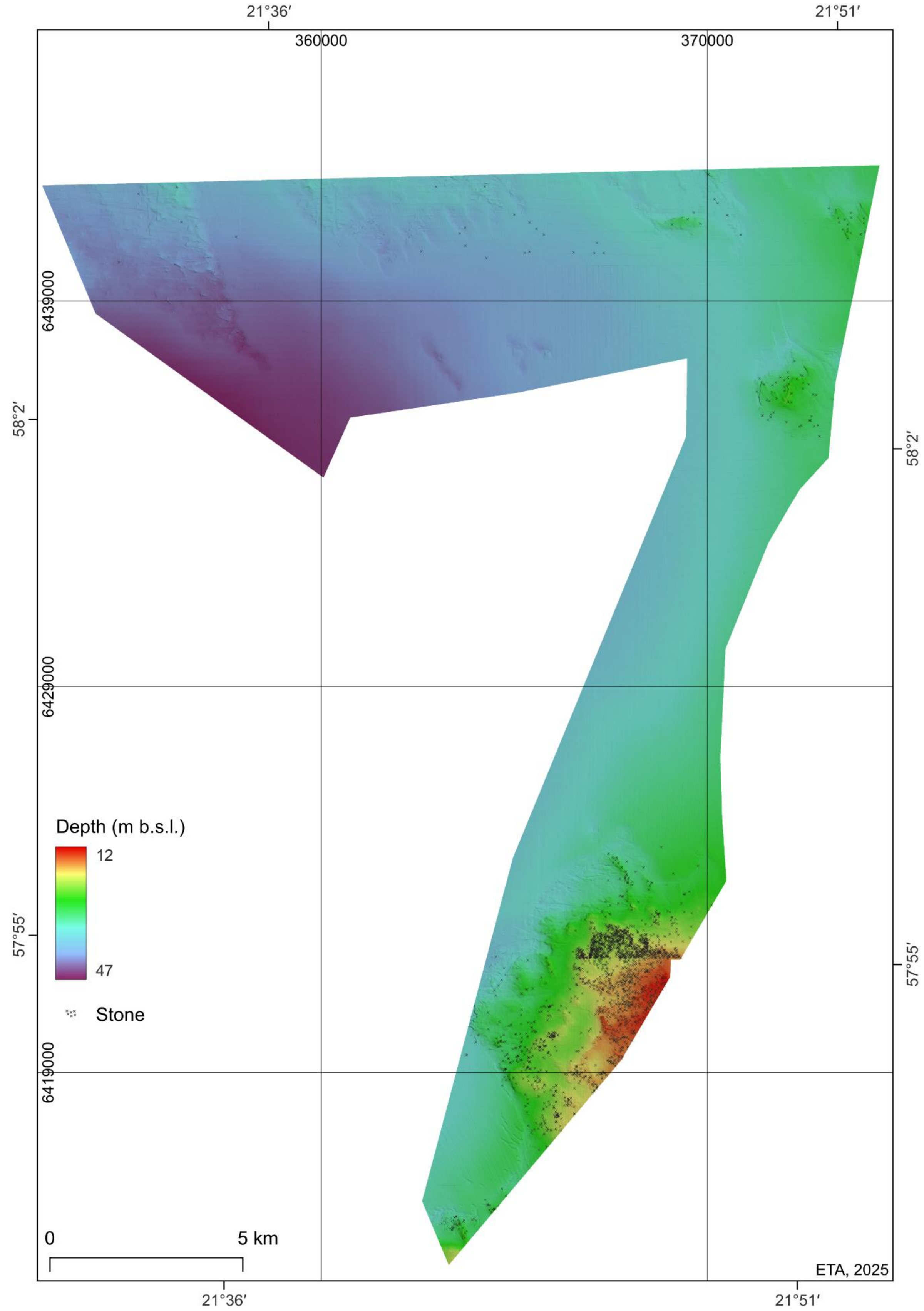

Fig. 7. Bottom relief features with detected seafloor boulders of the WFA based on multibeam echo-sounding data

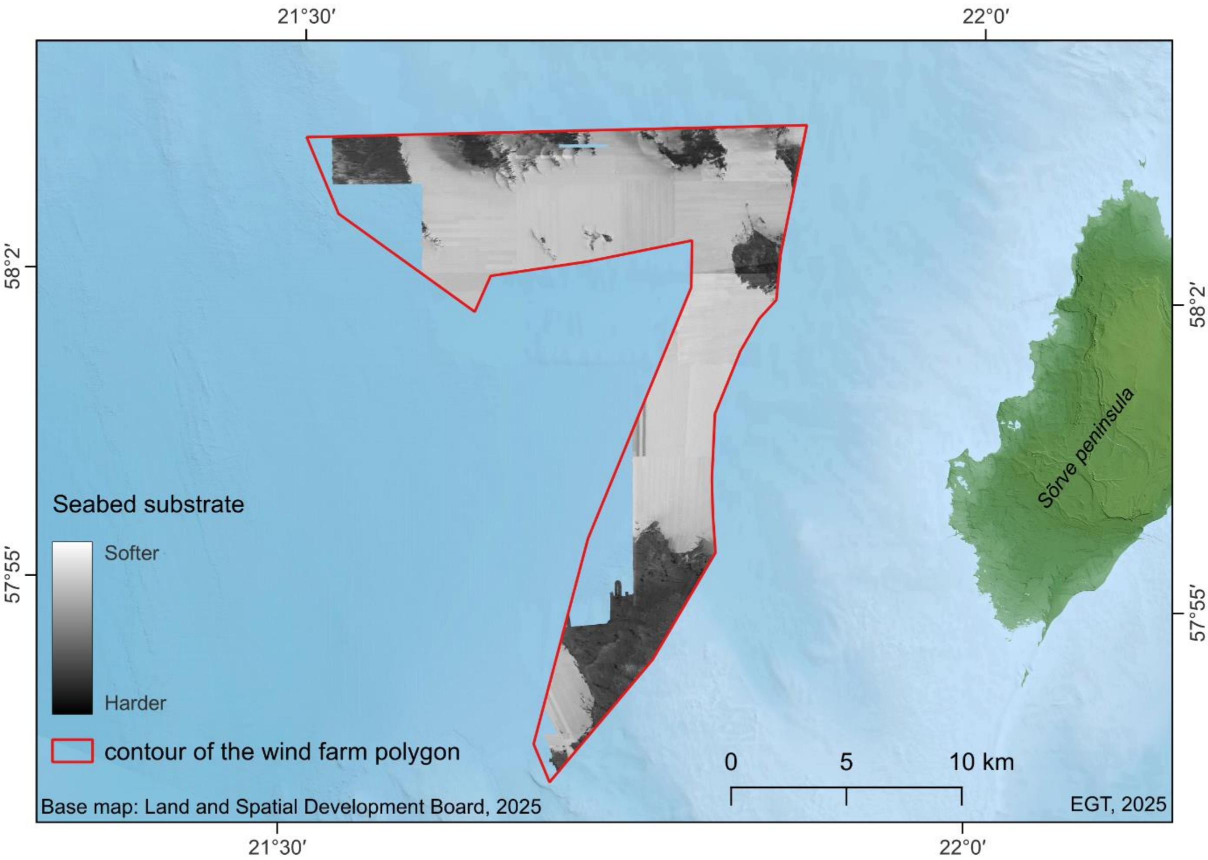

Fig. 8. Seabed substrate image of the WFA based on multibeam backscatter intensity data. Soft Baltic Sea sediments and the bedrock (covered to a lesser or greater extent by glacial till/waterlain glacial diamicton) are exposed on the seafloor within the light and dark areas, respectively

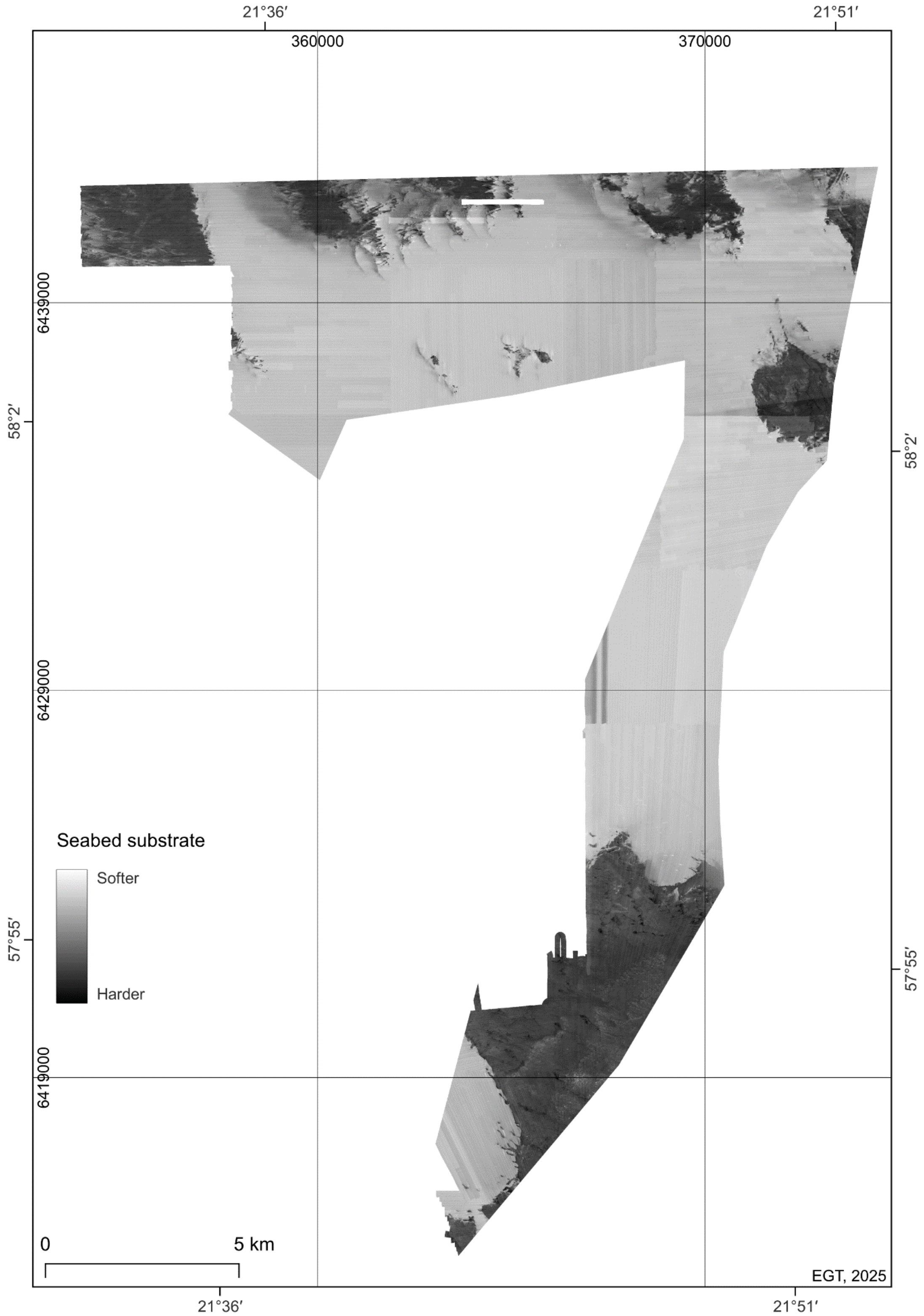

Fig. 8A. Enlarged excerpt from Fig. 8 showing more in detail the seabed substrate of the WFA drawn based on multibeam backscatter data. Soft Baltic Sea sediments and hard rocks/sediments (bedrock covered to a lesser or greater extent by glacial till/waterlain glacial diamicton) are exposed on the seafloor within the light and dark areas, respectively

1.4. The bedrock

1.4.1. The bedrock sequence exposed in and around the WFA off the Sõrve peninsula

Detailed lithostratigraphic subdivision and correlation scheme of the Silurian stratal sequence along the western coast of Saaremaa has been worked out based on numerous drill cores/outcrops onshore (Fig. 9). Based on the lithological and paleontological data, Saaremaa remains into the north-easternmost corner of the epicontinental Baltic Silurian basin, where the shallow-marine (open shelf, shoal, occasionally even lagoonal) facies dominate (Figs 9, 10). According to the seismic correlation scheme, shallow-marine facies belts with formations described on western Saaremaa extend across the WFA towards the central Baltic Sea (Figs 9-11). Thus, according to the compiled geological map, the Silurian Paadla, Kuressaare, Kaugatuma and Ohesaare formations crop out on the seafloor offshore the Sõrve peninsula in and around the WFA (Fig. 11).

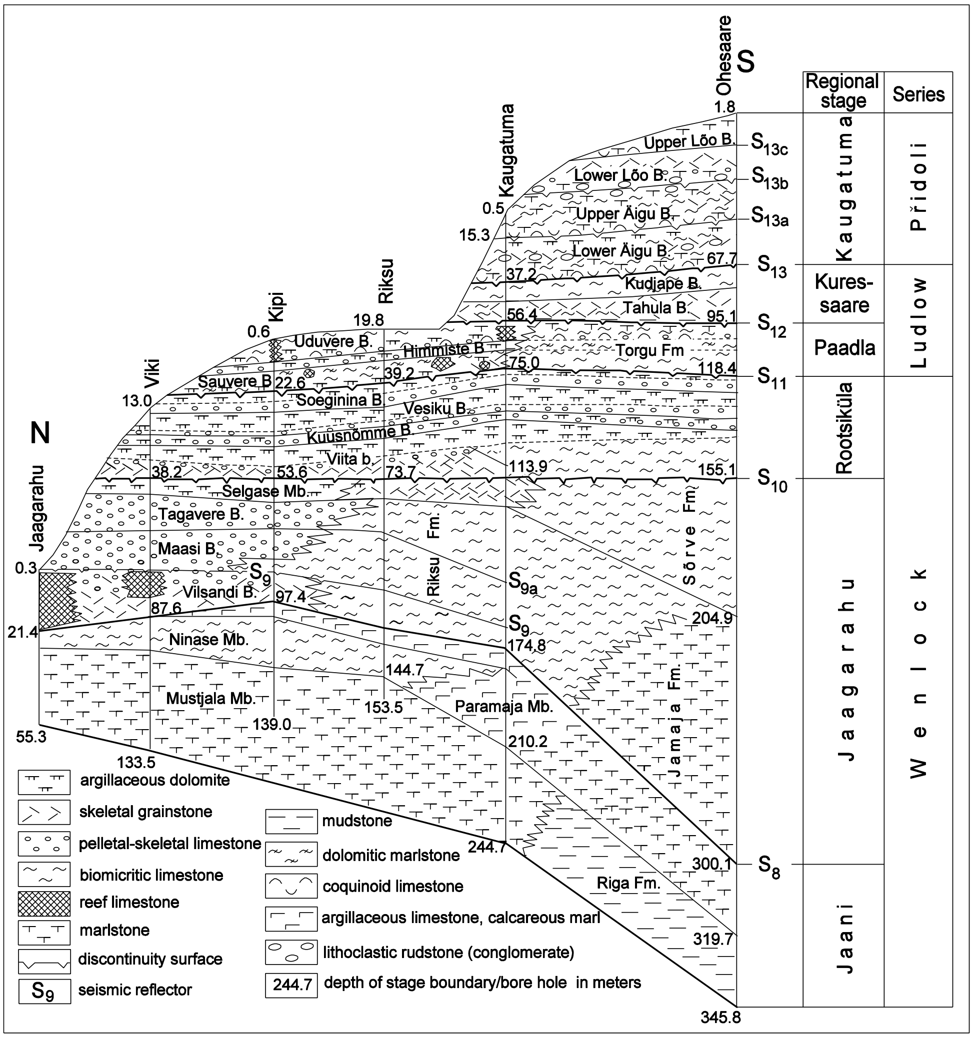

Fig. 9. Detailed geological cross section based on drill cores with distinguished Silurian formations (Fm) or Members (Mb) along the western coast of Saaremaa and their correlation with the offshore seismic reflectors S8-S13c drawn in Fig. 11 (modified after Nestor, 1997). For the location of the Jaagarahu-Ohesaare section, see Figs 11 and 12

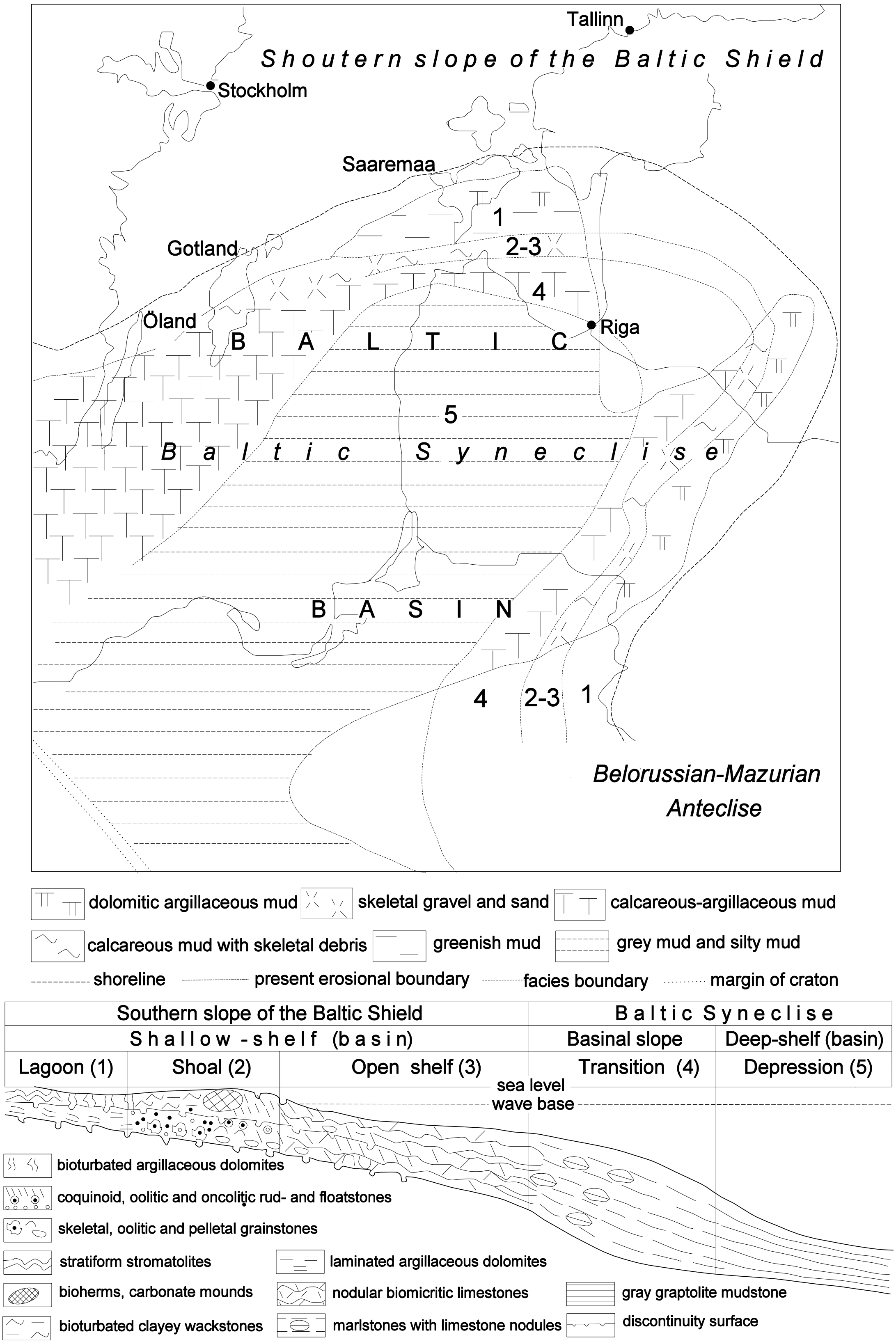

Fig. 10. General facies model of the Paleobaltic Silurian basin (below) and paleogeography with the location of the facies belts in respect to Saaremaa during the Jaagarahu-Rootsiküla time (above) (Tuuling & Flodén, 2011)

According to lithological/paleontological data, various bioclastic pelletal and argillaceous limestones with occasional coral-stromatoporoid bioherms of the shoal facies belt represent the Paadla formation. The Kuressaare and Kaugatuma formations formed in a deeper, open-shelf facies zone of the Paleobaltic Silurian basin (Figs 9, 10). Thus, more clayey and easily erodible biomicritic/bioclastic argillaceous limestones and marlstones represent the latter formations. The Ohesaare Formation that formed in open shelf conditions consists largely of argillaceous dolomitic marlstones or calcareous mudstones with thin interlayers of limestones.

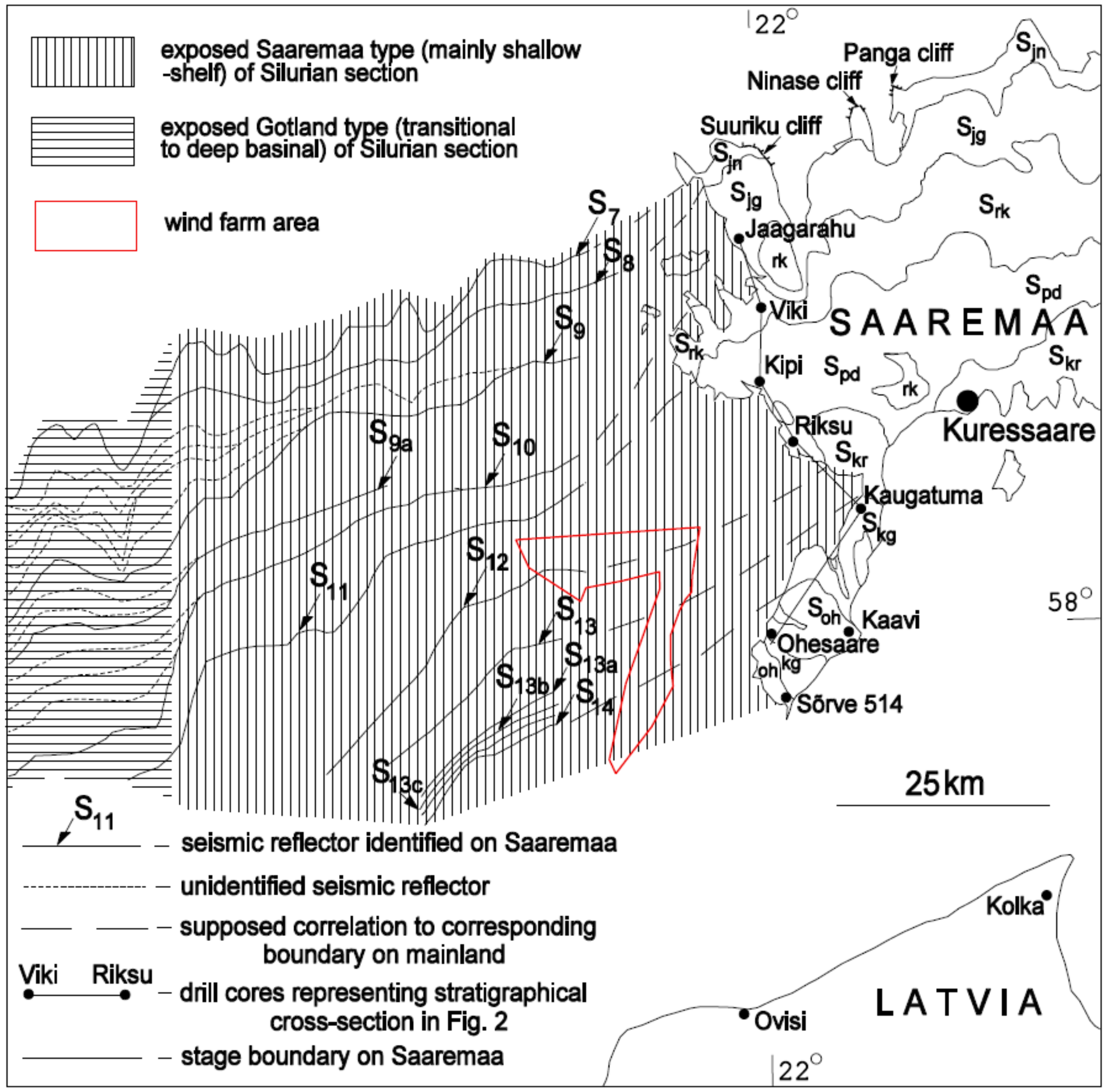

Fig. 11. Geological map with the 7-shaped wind farm polygon showing the correlation of the on- and offshore Silurian sequences around western Saaremaa (modified after Tuuling & Floden, 2011). Abbreviations of the Silurian (S) stages jn – Jaani, jg -Jaagarahu, rk - Rootsiküla, pd - Paadla, kr - Kuresaare, kg – Kaugatuma, oh – Ohesaare. For stratigraphic positions of the seismic reflectors, see Fig. 9

1.4.2. Outlines of the bedrock relief offshore western Saaremaa and around the WFA

As already described, the patches of outcropping bedrock covered with a thin layer of glacial till or possibly with postglacial ice lake clayey sediments emerging along the E and N borders of the WFA, were revealed by multibeam backscatter data (Figs 8, 8A). Some idea about the location of the bedrock surface along the shallow marine eastern margin of the WFA can be occasionally assumed also from the chirp-type seismo-acoustic profiles that are discussed below (in the chapter of the Quaternary sequence). However, it must be emphasized that the seismo-acoustic impulse of a chirp-type transmitter normally reaches only the glacial till surface (does not penetrate it) and therefore does not allow to determine and follow the bedrock surface.

The only specific bedrock data from the WFA originates from the early 1990s, when the Swedish-Estonian scientific team studied the bedrock sequence of the central Baltic Sea by means of the single channel analogue method using a low frequency (250–500 Hz) airgun transmitter. However, due to the poor quality (intricate shape of the seismic pulse, noise by shallow water multiples, etc.) the exact bedrock depth estimations on these analogue airgun recordings may vary considerably (occasionally even more than 5 m). In places, especially in the shallow marine areas like off western Saaremaa, exact following of the bedrock surface was even impossible due to shallow-water multiples. Furthermore, because the DECCA Navigator System was used at that time, positioning inaccuracy on the sea along the profiles could reach more than 50 m. Nevertheless, the profiles from early 1990s provide us so far the best, albeit rough values of bedrock depths and thus a general overview about the bedrock relief offshore western Saaremaa and around the WFA.

In all, eight profiles from early 1990s traverse/cover more or less also the WFA off the Sõrve peninsula (Figs 12–20). The position of the WFA in respect with the general background of the submarine bedrock relief offshore western Saaremaa becomes best evident on three long profiles (9301, 9107 and 9302) extending north-southerly across all offshore area of the island (Figs 12–15). Thus, two extensive bedrock relief entities emerge offshore the western coast of Saaremaa: 1) relatively flat (slightly undulating), about 30–40 km wide limestone plateau in the north that, 2) transfers to the southerly declining bedrock slope and depression near the Sõrve peninsula further to the south. The slightly undulating limestone plateau, which remains largely between the outcropping S_7 (marks also the location of the Silurian Klint in Figs 13 and 15) and S_{12} reflectors on the geological map (Fig. 11), has largely formed along the hard, erosion-resistant pure limestones of the Jaagarahu, Rootsiküla and Paadla formations. The southerly declining bedrock slope and depression, however, are carved into the clay-rich soft and easily erodible limestones of the Kuressaare, Kaugatuma and Ohessaare formations (Figs 9–11). The multibeam backscatter map (Figs 8 and 8A) supports the latter claim, as patches with the hard bottom substrate (limestone/glacial till outcrops possibly covered with a thin layer of waterlain glacial diamicton) exposed along the northern margin of the E-W extending section of the wind farm polygon, remain largely within the area of the outcropping Paadla rocks (Fig. 11).

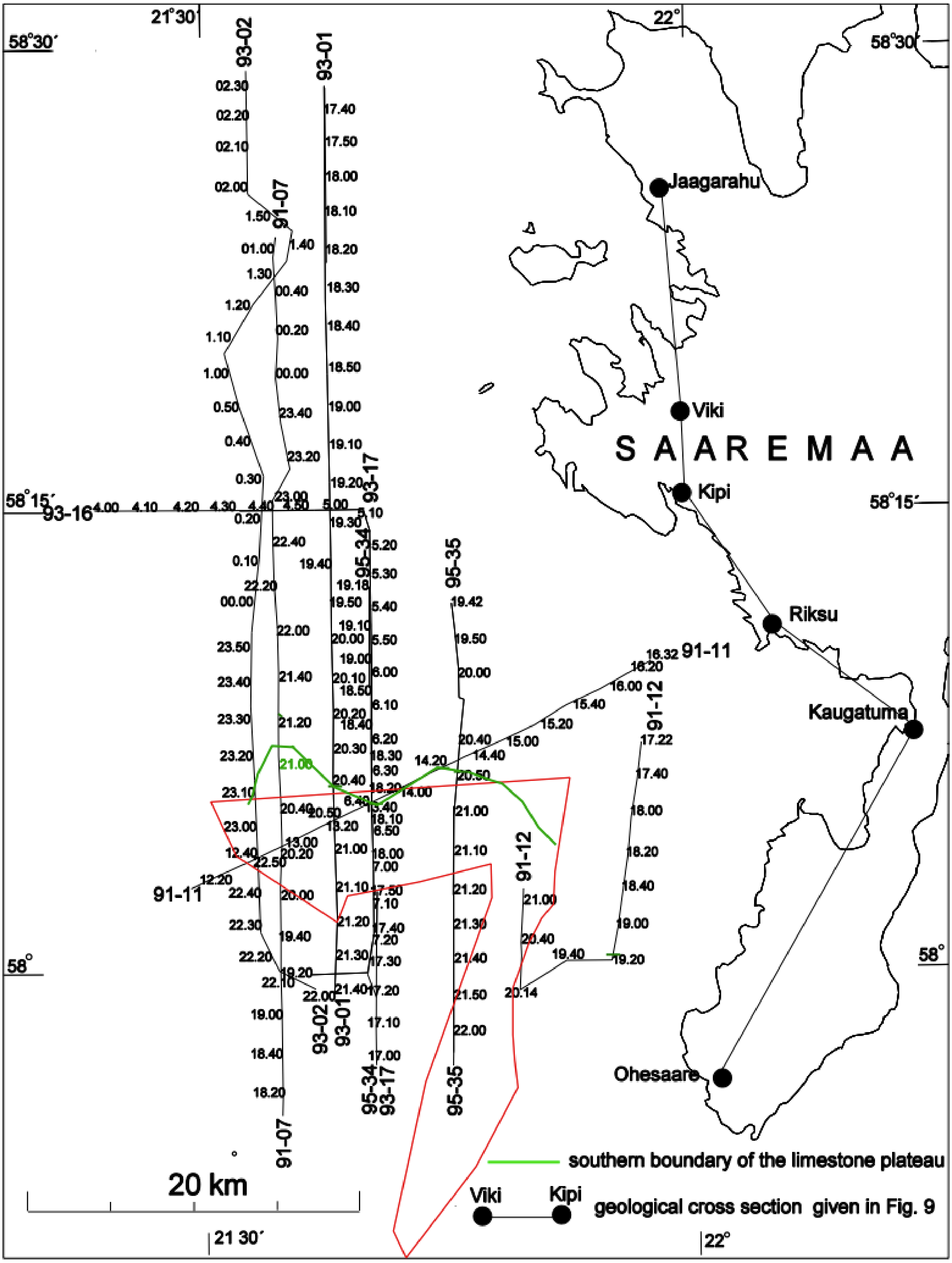

Fig. 12. Seismic airgun profiles from the early 1990s covering the 7-shaped wind farm polygon offshore western Saaremaa

The southern boundary of the limestone plateau sketched based on scarce airgun data (Fig. 12) indicates that the northern margin of the WFA is located around the area where the bedrock plateau in the north transfers to the southerly deepening bedrock slope. Still, about 3–8 km wide and 20 km long E-W extending northern segment of the WFA rests largely on the southerly slanting bedrock slope buried under a thin, southwards thickening Quaternary cover. This is seen also in most of the interpreted airgun profiles (Figs 13–20) and verified by chirp-type seismo-acoustic data presented in the Quaternary chapter. The bedrock slope with slightly undulating surface is occasionally notched by valley-like incisions (Figs 16, 17 and 20) and obviously descends to a larger bedrock depression further to the south. This depression emerges in the profile 95-35 (Fig. 18) and is partially seen in the profiles 93-02, 91-07, 95-34 (Figs 13, 14 and 16). The absolute elevation of the limestone plateau north of the WFA, covered largely with a thin (a few up to 5 m) layer of glacial till or waterlain glacial diamicton, remains chiefly at about 20–30 m b.s.l. (Figs 13–15). The inflection point between the bedrock plateau and slope occurs largely around 40 m b.s.l. Within the slope, the elevation of the bedrock falls gradually southwards and reaches about 80–90 m b.s.l. further to the south of the WFA (profile 95-34 in Fig. 14). Exceptionally, the latter depth emerges also on the bottom of a solitary valley-like incision carved into the bedrock slope around the southern margin of the E-W trending northern section of the wind farm polygon (profiles 95-34 and 93-17 in Figs 16 and 17). As it became evident already from the multibeam backscatter map (Figs 8 and 8A), the bedrock depression alongside its southerly descending slope is buried under postglacial Baltic Ice Lake (varved) clays, differently from the limestone plateau areas in the north and east. Due to the tilted slope area and valley-like incisions, the elevation of the bedrock surface within the WTA can vary considerably. The depth of the bedrock varies largely between 40–60 m b.s.l. in the limits of the slope. In the northern part of the WFA, partially located on the southern margin of the limestone plateau, the bedrock can rise to 35–40 m b.s.l. (Figs 15, 18 and 20). However, the deepest bedrock value > 80 m b.s.l. occurs at the bottom of a solitary slope cutting a valley emerging around the southern margin of the E-W trending segment of the wind farm polygon (Figs 16 and 17). Airgun profiles indicate that down the slope increasing thickness of the Quaternary sediments remains largely within 20 m. However, the total thickness of the Quaternary cover can reach about 40 m in the bedrock depression further south of the WFA, as well as in the valley-like incisions at the southern margin of the E-W trending segment of the wind farm polygon (Figs 16 and 17).

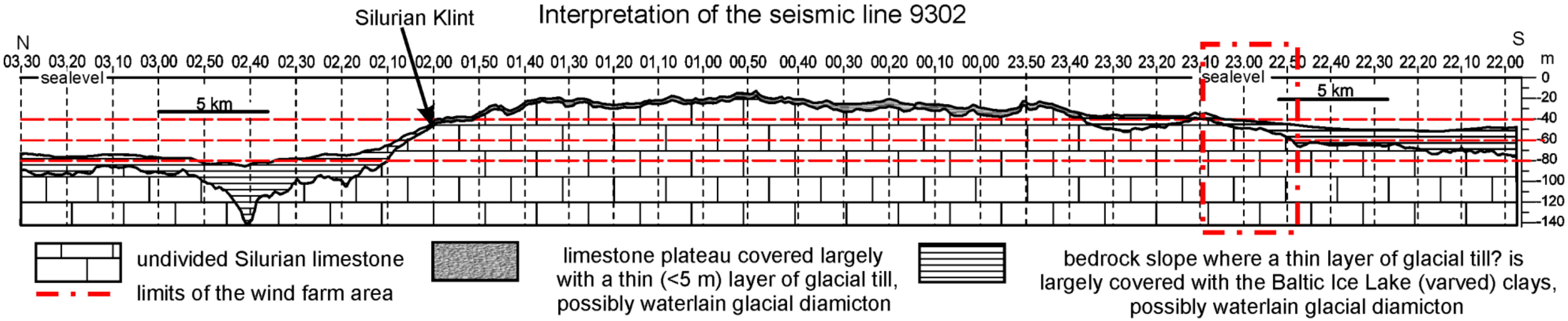

Fig. 13. Interpretation of the seismic line 93-02. For location of the line with its shot-points, see Fig. 12

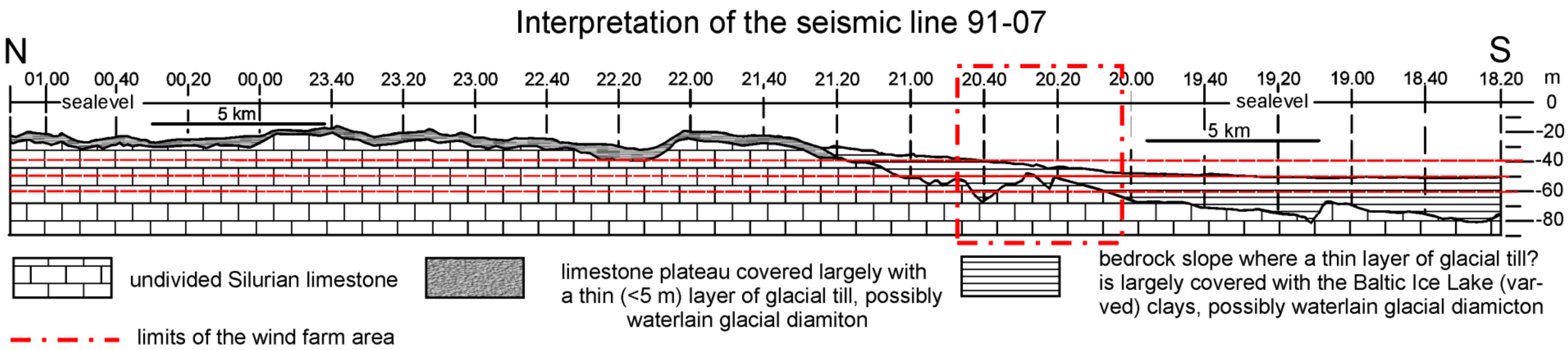

Fig. 14. Interpretation of the seismic profile 91-07. For location of the line with its shot-points, see Fig. 12

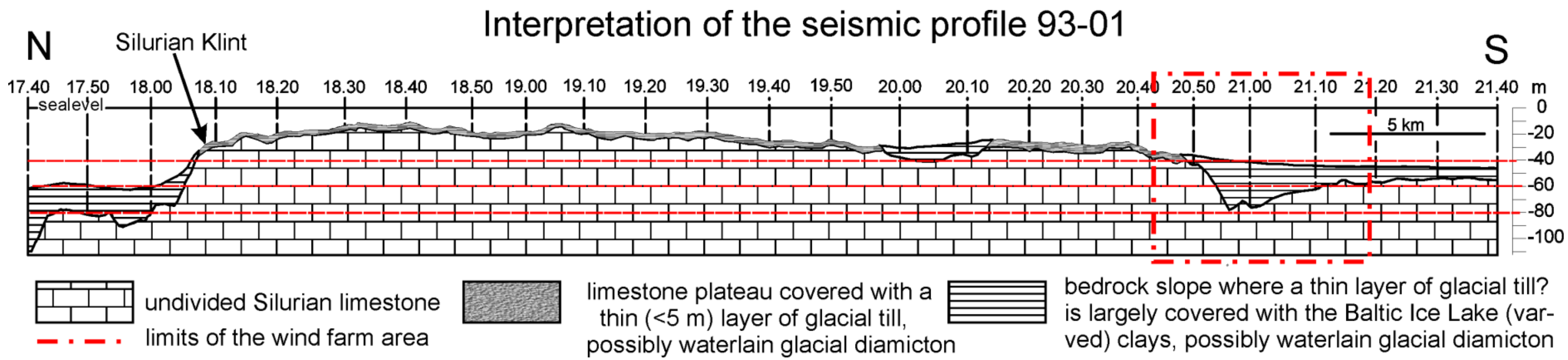

Fig. 15. Interpretation of the seismic profile 93-01. For location of the line with its shot-points, see Fig. 12

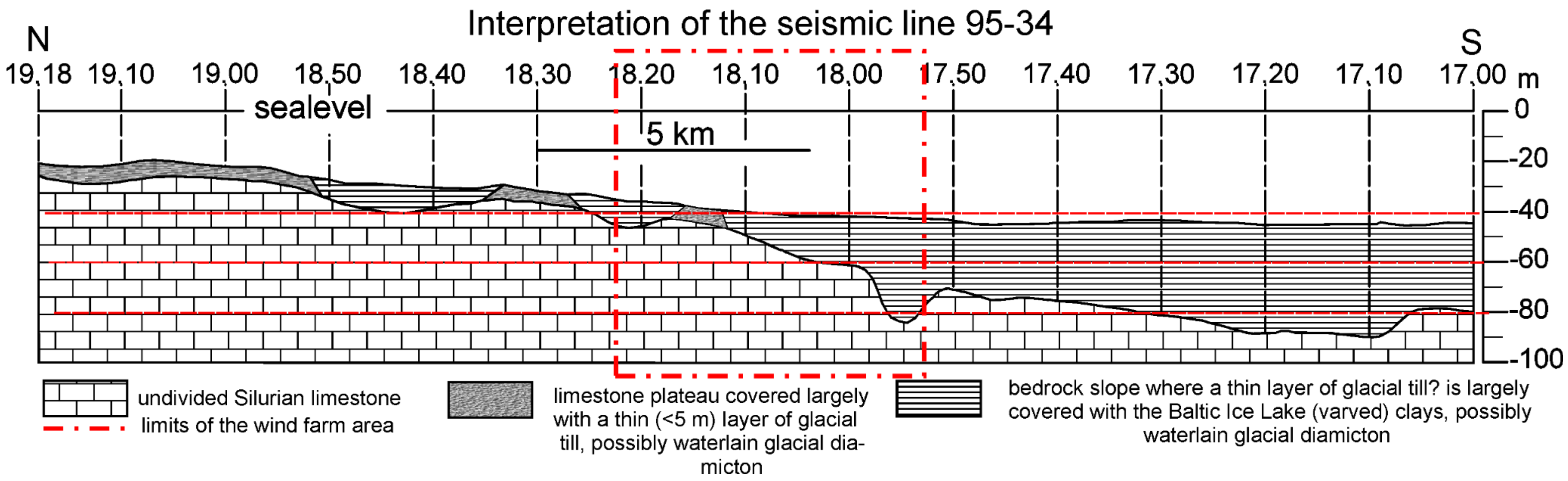

Fig. 16. Interpretation of the seismic profile 95-34. For location of the line with its shot-points, see Fig. 12

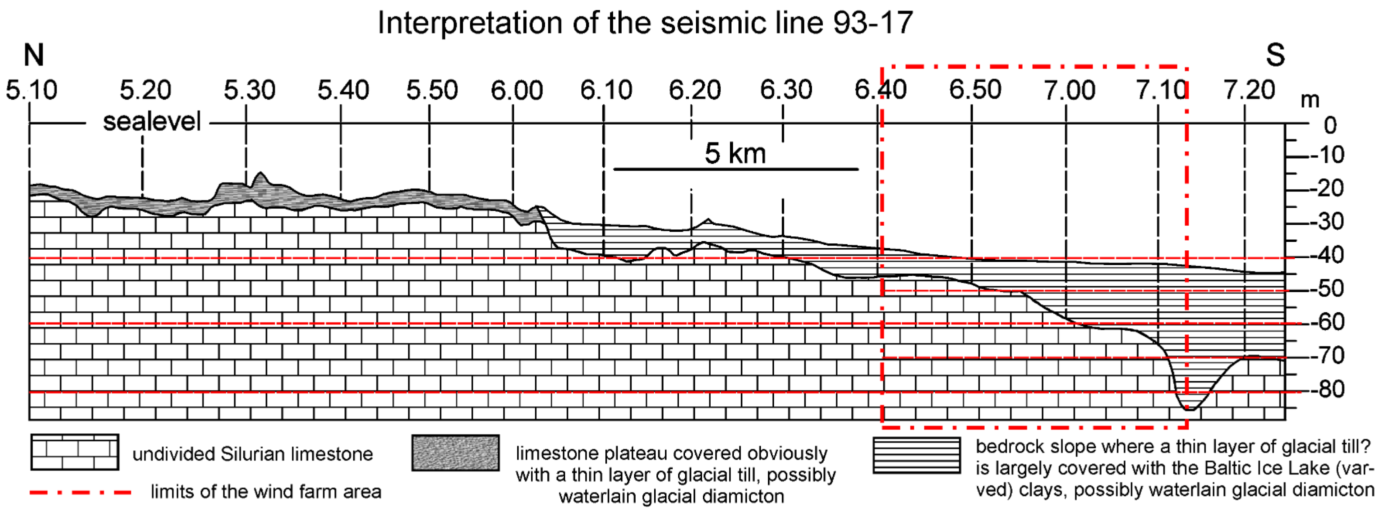

Fig. 17. Interpretation of the seismic profile 93-17. For location of the line with its shot-points, see Fig. 12

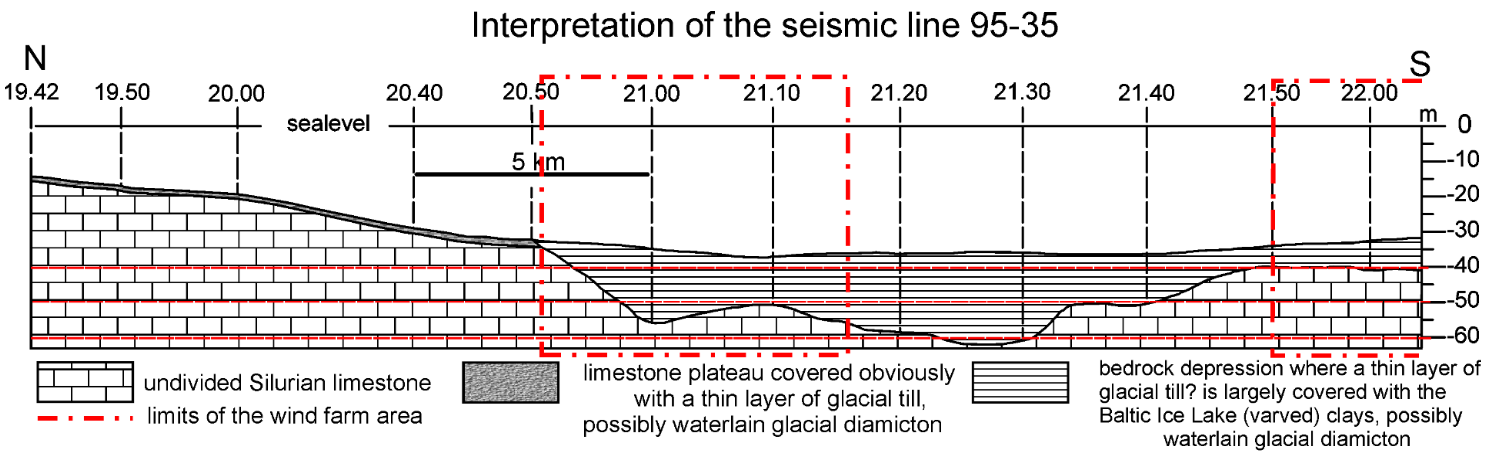

Fig. 18. Interpretation of the seismic profile 95-35. For location of the line with its shot-points, see Fig. 12

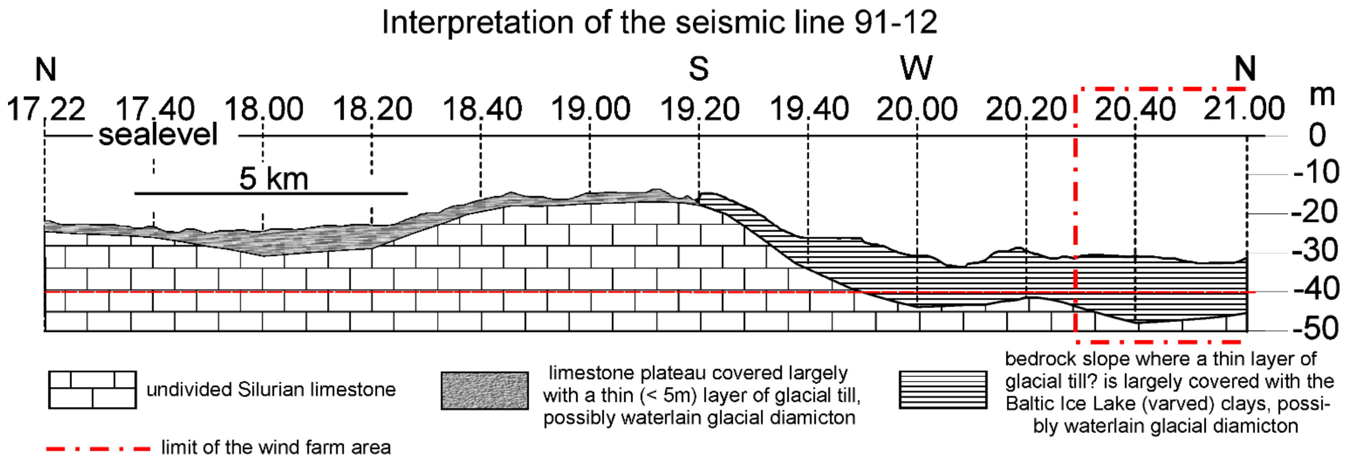

Fig. 19. Interpretation of the seismic profile 91-12. For location of the line with its shot-points, see Fig. 12

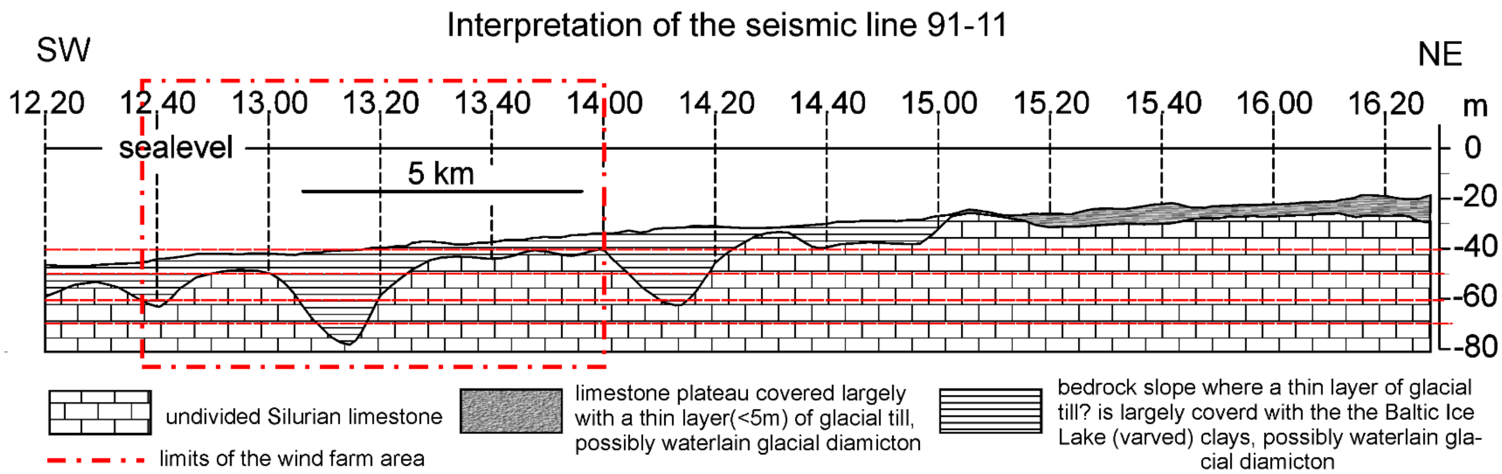

Fig. 20. Interpretation of the seismic profile 91-11. For location of the line with its shot-points, see Fig. 12

1.5. The Quaternary sequence

1.5.1. Net of the chirp produced seismo-acoustic lines covering the WFA

During the years 2017–2024, the Estonian Maritime Administration covered the area off the Sõrve peninsula with a dense set of seismo-acoustic profiles (Fig. 21) using a 2–9 kHz chirp-type transmitter. These so far uninterpreted good-quality digital profiles gave us a possibility to study more closely the Quaternary sequence, its subdivision and thickness around the WFA. The pulse of a chirp-type transmitter normally bounces entirely back from a glacial till surface, i.e. from the layer that in the onshore, as well as offshore areas of Estonia normally covers the bedrock. Thus, this method normally allows to determine only the surface of the glacial till and study the younger postglacial Baltic Sea (Baltic Ice Lake, Yoldia Sea, Ancylus Lake and Litorina Sea) sediments above it.

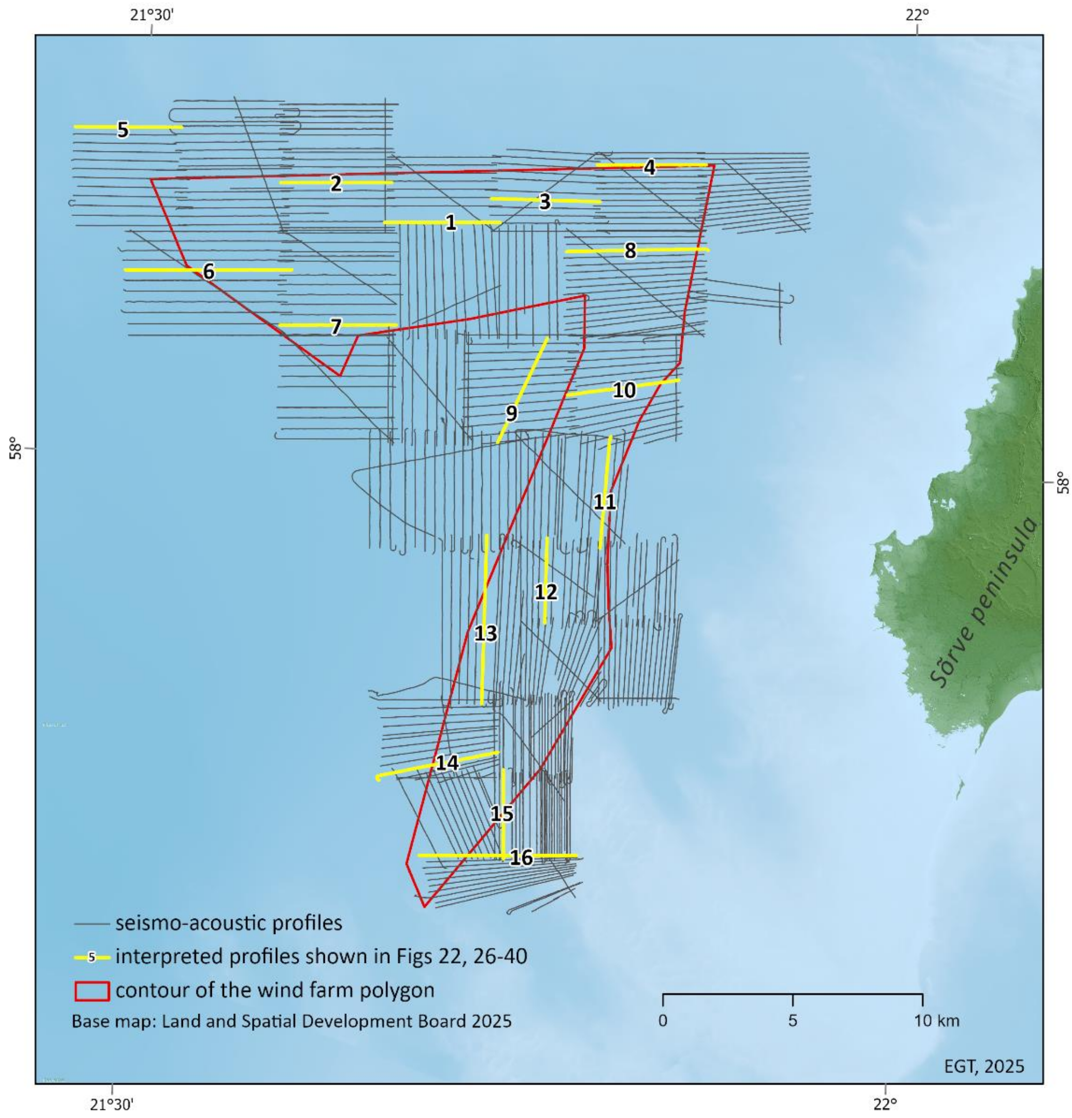

Fig. 21. Map showing the net of the seismo-acoustic (Chirp) profiles and locations of the interpreted profiles offshore the Sõrve peninsula

1.5.2. Difficulties in distinguishing the bedrock and glacial till surfaces

If the layer of glacial till is missing or is insignificant in thickness, instead of recording its surface the pulse of a chirp-type transmitter detects the seismo-acoustically impenetrable upper boundary of the bedrock. In this case it is not unambiguously certain, which one of the two surfaces emerges on the seismo-acoustic recordings. Based on the multibeam backscatter and also chirp-type profiles data, some areas around the WFA are likely missing the typical glacial till sediments. This concerns principally the areas with a more elevated bedrock surface, i.e. the areas near the limestone plateau surrounding the earlier described bedrock depression. However, similar areas might emerge also within the bedrock depression, although there are some signs in the airgun, as well as in the chirp-type profiles indicating presence of some glacial till sediments in the deeper bedrock areas of the WFA. To get reliable information about the possible distribution and thickness variations of the glacial till layer around the WFA, a special study is needed where the chirp- and the boomer type transmitters (the pulse of which penetrates the glacial till) are operated simultaneously. Juxtaposing recordings generated by these two transmitters normally helps to distinguish and determine unmistakably the glacial till and bedrock surfaces, and thus follow the glacial till layer between them. As no recordings from a boomer-type transmitter are available, it is problematic to unambiguously distinguish between the glacial till and the bedrock surfaces around the WFA. Since the seismo-acoustically impenetrable reflector level in our chirp-type recordings can reflect the upper boundary either of the bedrock or the glacial till, in our study it is treated as the surface of glacial till or bedrock.

1.5.3. Interpretation of the seismo-stratigraphic units emerging in the chirp-type profiles around the WFA

Still, in rare cases, the pulse of a chirp-type transmitter can penetrate the glacial till layer and reach even the underlying bedrock. Such rare occasion is possibly demonstrated in a profile from the northern part of the WFA, where an intermittent reflector emerges below the suggested glacial till surface (Fig. 22). Besides the possible bedrock and glacial till surfaces, two more or less distinctive reflectors separating different seismic signatures, or lithological units, emerge in this profile. Stratigraphic position of the upper one in the section, which by the bedrock depression largely coincides with the seafloor, is easily identifiable and marks the upper boundary of the Baltic Ice Lake varved clay unit (Fig. 22). Another, strongly undulating reflector at the base of the varved clay layer marks the upper boundary of a problematic unit overlying the glacial till. As there are no drilling data offshore the Sõrve peninsula, the exact genesis and lithological content of this unit remains unclear, since normally the glacial till is covered by the Baltic Ice Lake varved clay complex. However, the seismo-acoustic signature of this problematic unit transparent for a chirp-type transmitter resembles a “dirty” clay layer, which unlike classical glacial till contains more clay and less gravel/pebble fractions. Thus, this problematic layer may represent waterlain glacial diamicton, a clayey complex containing small rock pieces and pebbles deposited from icebergs detached from glaciers. A similar layer has been followed in the seismo-acoustic profiles in the western part of the Gulf of Riga (Tsyrulnikov et al., 2012) and mapped also in the Väinameri Sea (Tuuling et al., 2022). Ripple marks on top of the varved clay unit emerging on numerous profiles (Figs. 22, 28) prove that the sea bottom in the bedrock depression area of the WFA is widely covered with loose sandy sediments that are easily moved by currents and waves.

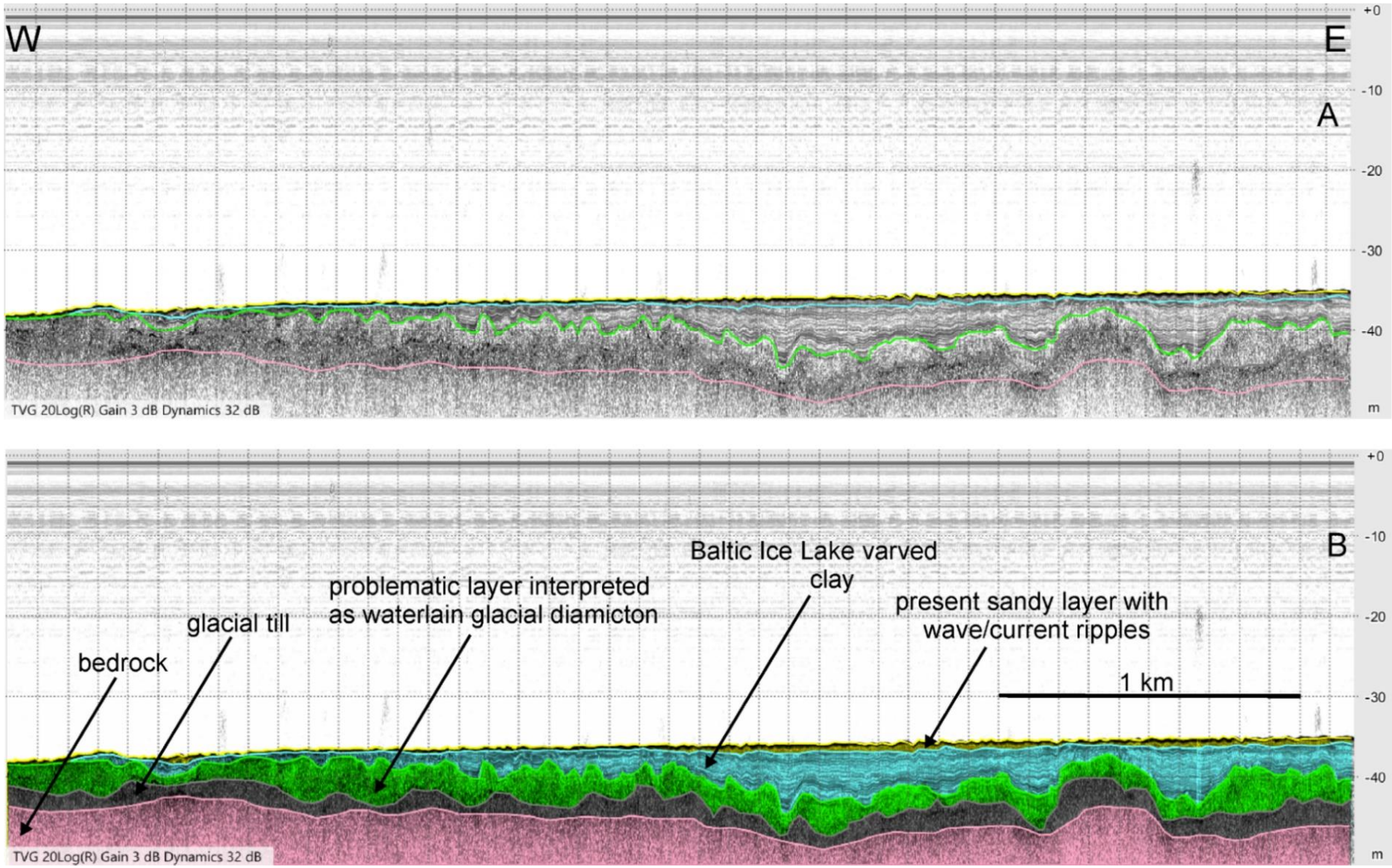

Fig. 22. Uninterpreted (A) and interpreted (B) versions of a chirp-type seismo-acoustic profile to demonstrate seismo-acoustic units emerging around the northern WFA offshore the Sõrve peninsula. In this profile, the pulse of a chirp-type transmitter exceptionally penetrates the glacial till unit and reveals occasionally the bedrock surface. For location of the profile, see profile 1 in Fig. 21

1.5.4. Examples of interpreted seismo-acoustic profiles and maps demonstrating the reliefs and thicknesses along different stratigraphic boundaries and units

As multibeam backscatter and echo sounding, as well as airgun data (Figs 6–8, 8A, 13 and 15) show, such areas where Quaternary sediments are insignificant in thickness or even absent emerge along the north and east margins of the E-W and NE-SW trending sections of the wind farm polygon, respectively. Thus, similar patches may expose the bedrock or areas where the bedrock is covered with some glacial till and, as deduced above, with a thin layer of the younger Baltic Sea sediments (waterlain glacial diamicton). In addition to the multibeam backscatter map (Figs 8 and 8A), areas with thin and substantial Quaternary cover (high- and low-lying areas) are excellently distinguished also on the relief map and 3D model of the problematic glacial till/bedrock surface (Figs 23 and 24), and on the thickness map of postglacial sediments drawn on the basis of chirp-type seismo-acoustic data (Fig. 25). Relying on these maps, the locations of chirp-type seismo-acoustic profiles are chosen (Fig. 21) to demonstrate and discuss subdivision, distribution and thicknesses of the Quaternary cover, foremost its postglacial portion in different areas around the WFA (Figs 26–40).

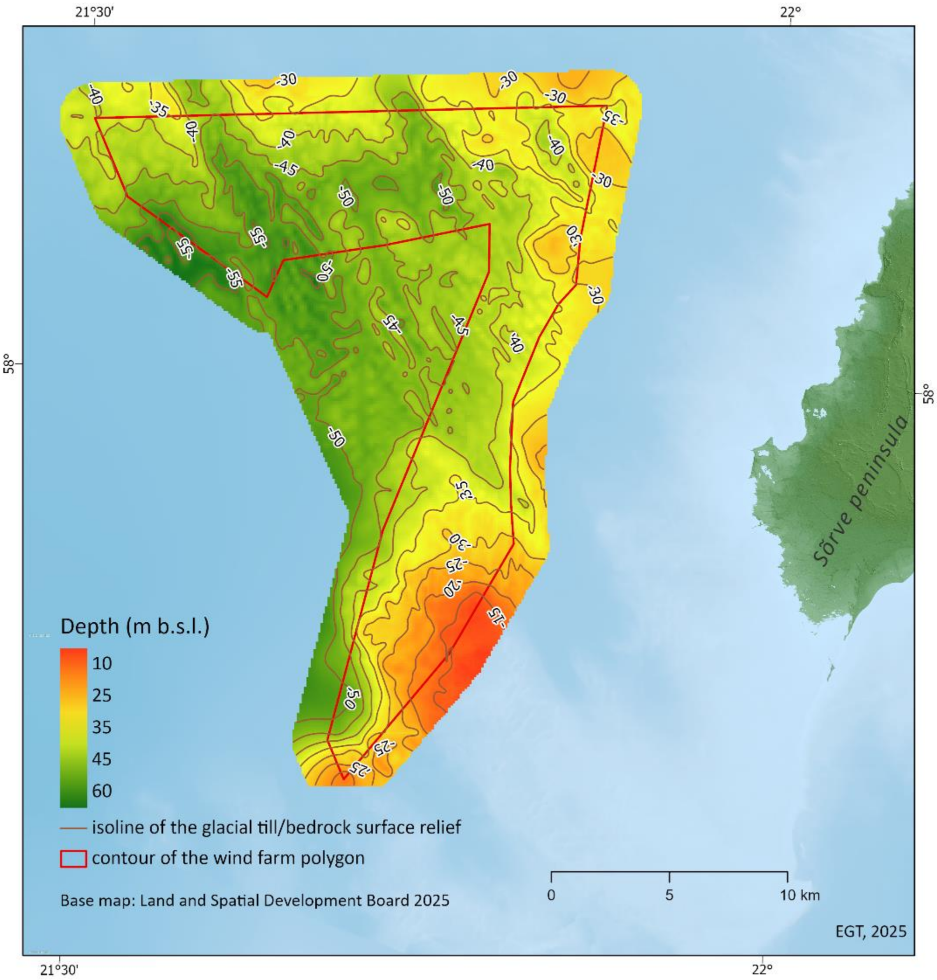

Fig. 23. Relief (depth) map along the problematical, seismo-acoustically impenetrable glacial till/bedrock surface around the WFA

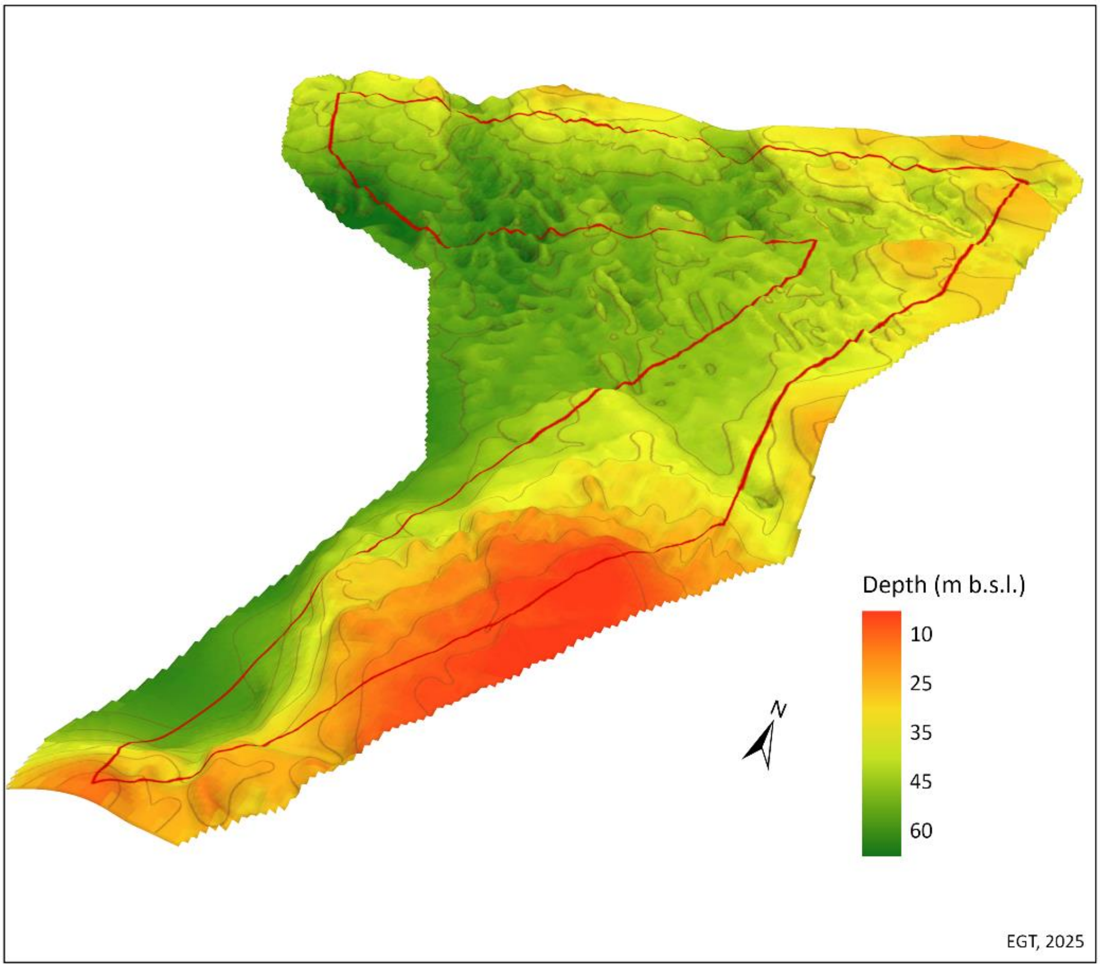

Fig. 24. 3D model showing the relief (depth) along the problematic, seismo-acoustically impenetrable glacial till/bedrock surface around the WFA

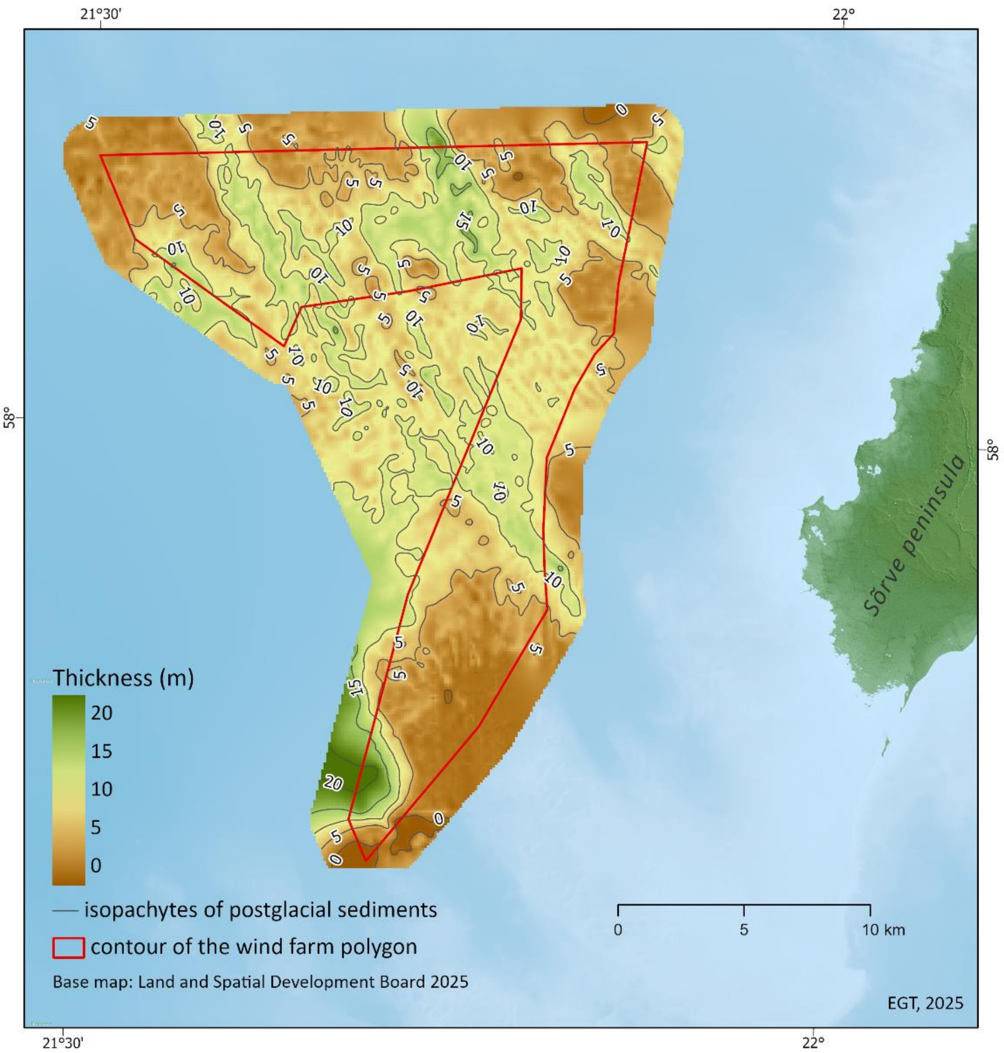

Fig. 25. Thickness map of postglacial sediments overlying the problematical glacial till/bedrock surface around the WFA

According to the seismostratigraphic subdivision of the chirp-type profiles (Fig. 22), two substantial postglacial Quaternary units emerge above the problematic glacial till/bedrock surface around the WFA (Figs 26–40). Both these clayey units, the waterlain glacial diamicton with some pebble/gravel fraction, as well as the pure varved clay complex overlying it, were obviously formed in glacial lake conditions. Although it is often difficult to identify the waterlain glacial diamicton in areas with a thin Quaternary cover (plateau areas with high bedrock relief), it is obviously ubiquitous over the WFA. The Baltic Ice Lake varved clay unit, however, has been deposited only in areas with a deeper bedrock relief, i.e. in bedrock depressions and valleys, where it is exposed also at the sea bottom. This becomes evident in all the interpreted seismo-acoustic lines (Figs 26-40), as well as on the map of Quaternary sediments of the WFA (Fig. 41). The thicknesses of the waterlain glacial diamicton and varved clay units alongside their changes and trends across the WFA are demonstrated on the corresponding maps (Figs 42 and 43). Thus, the thickness of the waterlain glacial diamicton ubiquitous over the WFA can vary almost from zero (in the areas with possible bedrock outcrops in Fig. 27) to 10 m in the bedrock depression around the southern corner of the WFA (Figs 38, 42). The thickness of the Baltic Ice Lake varved clay unit, which is absent in elevated bedrock plateau areas with thin Quaternary cover, can reach more than 10 m in deeper bedrock cuttings (depressions and valleys) located near the northern margin and around the southern corner of the wind farm polygon (Figs 27, 38, 40 and 43). The upper surface of the waterlain glacial diamicton, which outside the area of the outcropping varved clay unit (Fig. 41) coincides largely with the sea bottom, remains in the bedrock slope-depression area of the WFA largely within 40–50 m b.s.l. (Fig. 44).

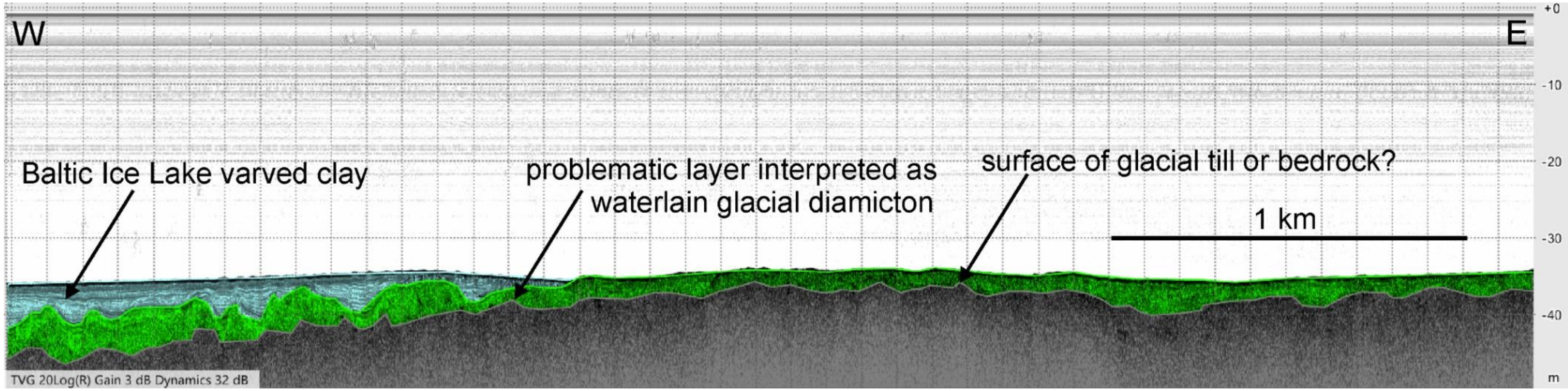

Fig. 26. Interpreted chirp-type seismo-acoustic profile from the northern part of the WFA. For location of the profile, see line 2 in Fig. 21

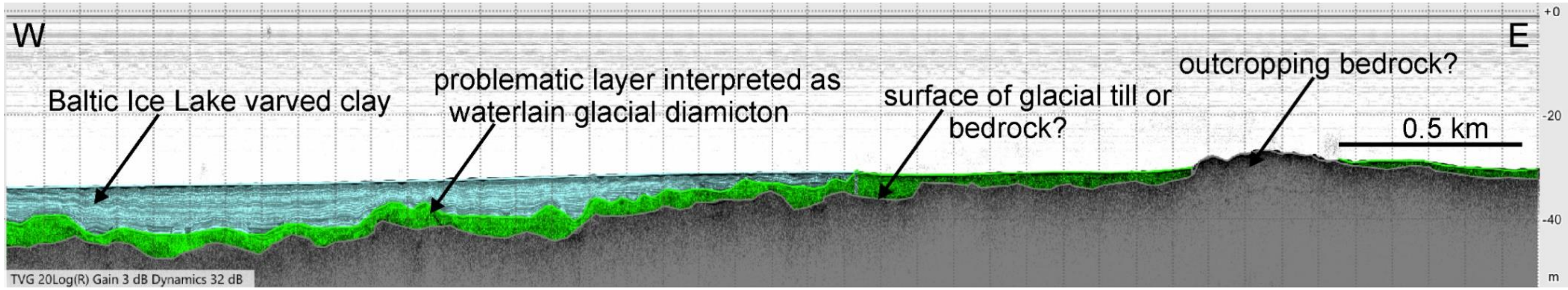

Fig. 27. Interpreted chirp-type seismo-acoustic profile from the northern part of the WFA. For location of the profile, see line 3 in Fig. 21

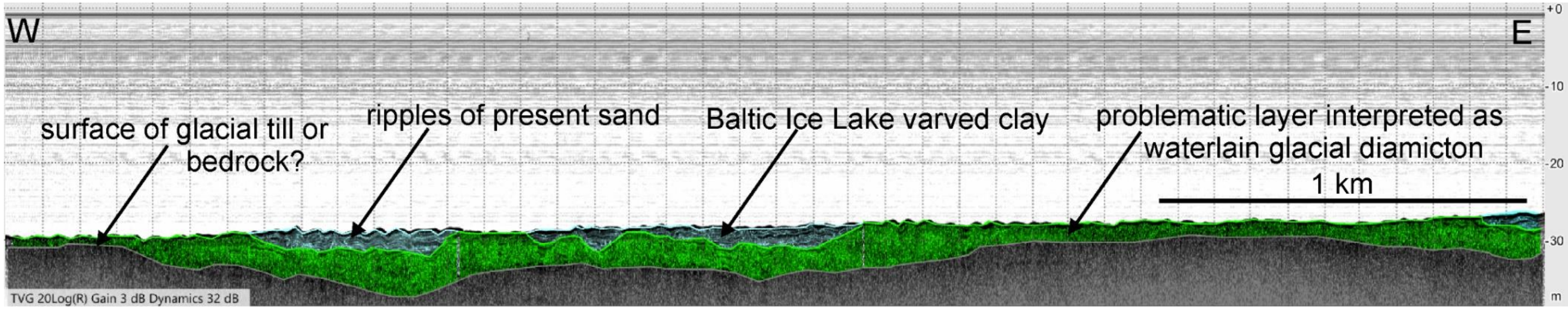

Fig. 28. Interpreted chirp-type seismo-acoustic profile from the northern part of the WFA. For location of the profile, see line 4 in Fig. 21

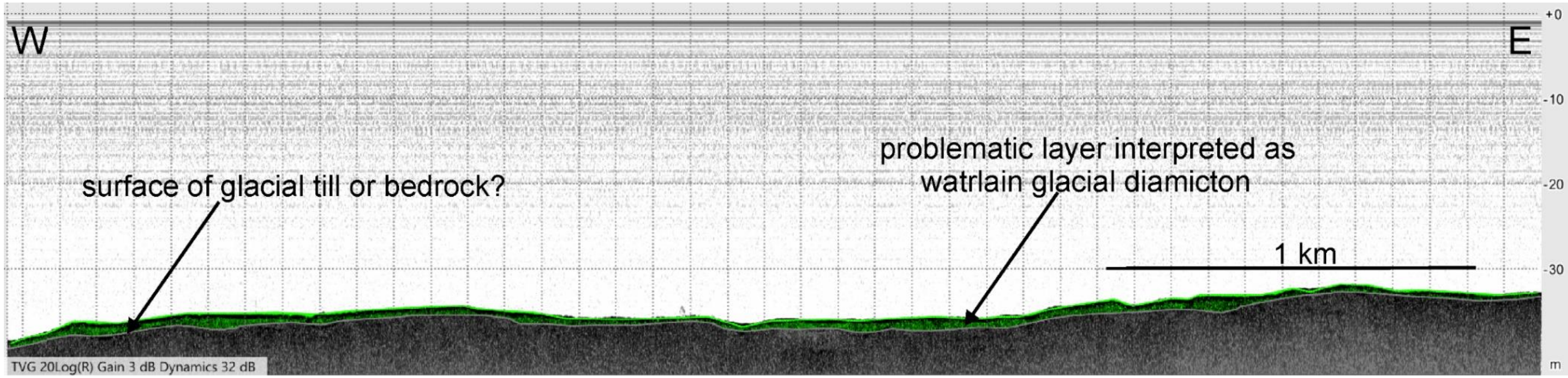

Fig. 29. Interpreted chirp-type seismo-acoustic profile located on the limestone plateau just outside the northern boundary of the WFA. For location of the profile, see line 5 in Fig. 21

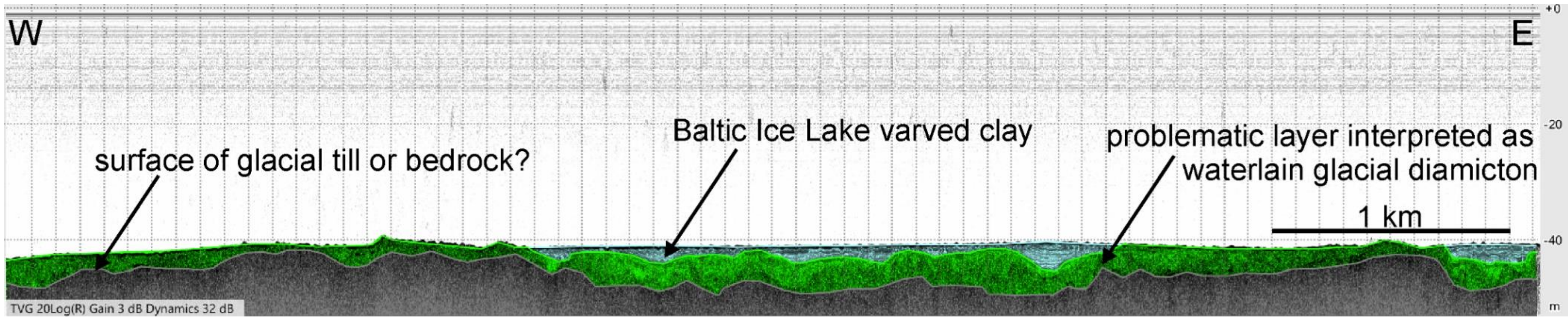

Fig. 30. Interpreted chirp-type seismo-acoustic profile from the northern part of the WFA. For location of the profile, see line 6 in Fig. 21

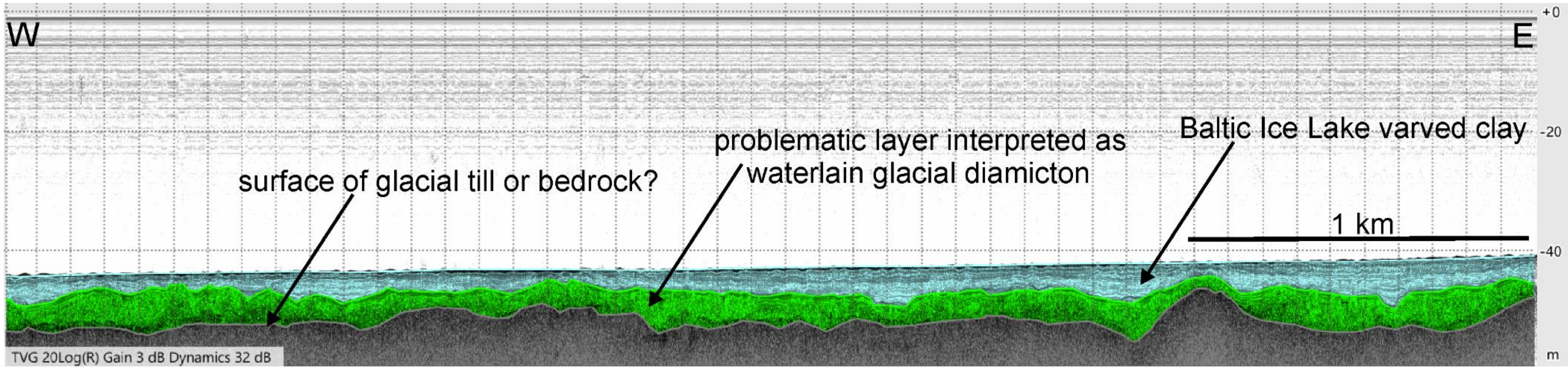

Fig. 31. Interpreted chirp-type seismo-acoustic profile from the northern part of the WFA. For location of the profile, see line 7 in Fig. 21

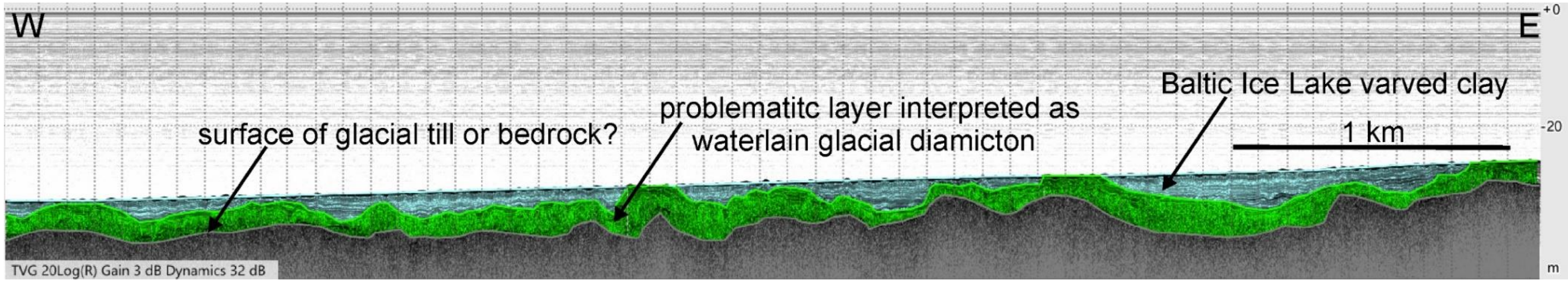

Fig. 32. Interpreted chirp-type seismo-acoustic profile from the northern part of the WFA. For location of the profile, see line 8 in Fig. 21

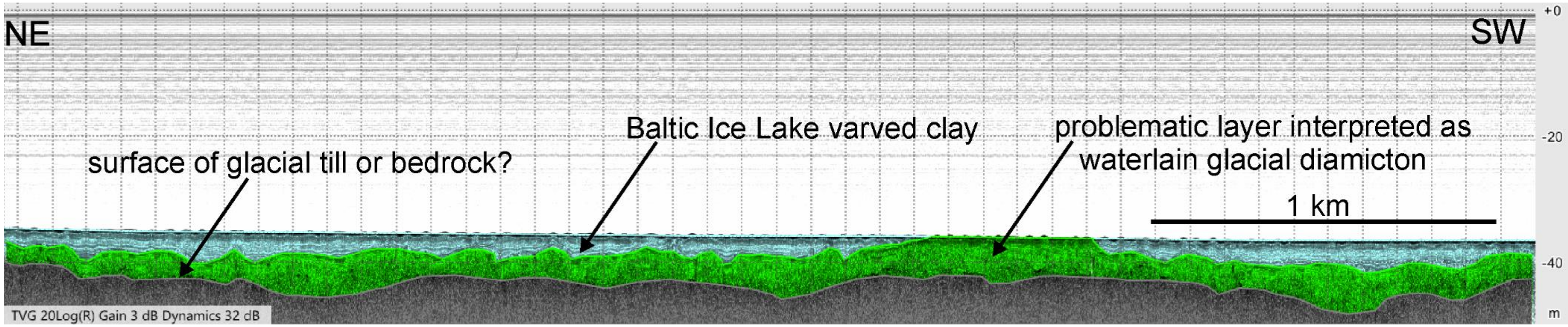

Fig. 33. Interpreted chirp-type seismo-acoustic profile from the central part of the WFA. For location of the profile, see line 9 in Fig. 21

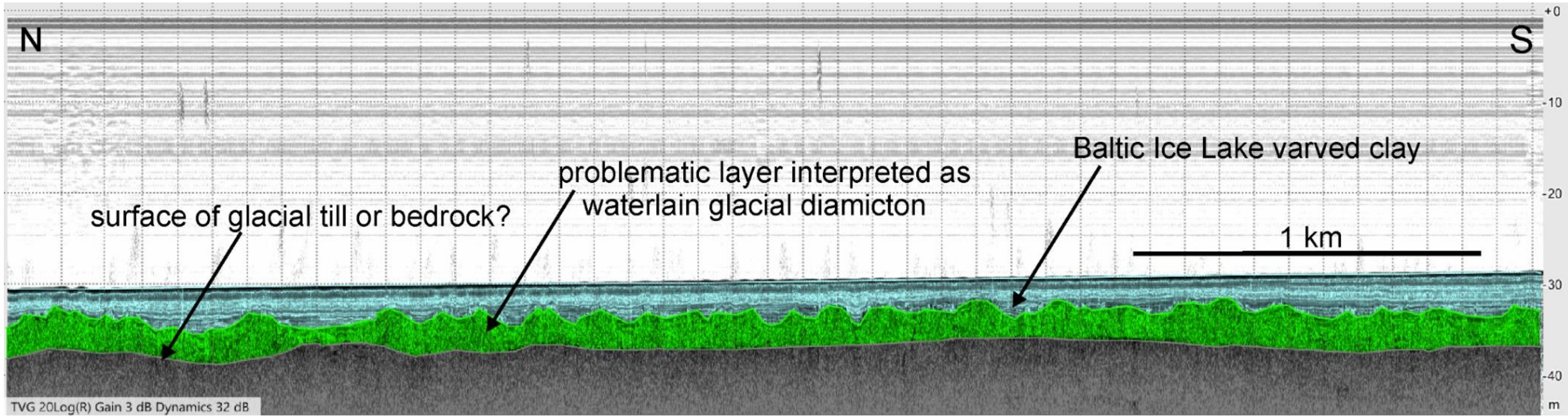

Fig. 34. Interpreted chirp-type seismo-acoustic profile from the central part of the WFA. For location of the profile, see line 10 in Fig. 21

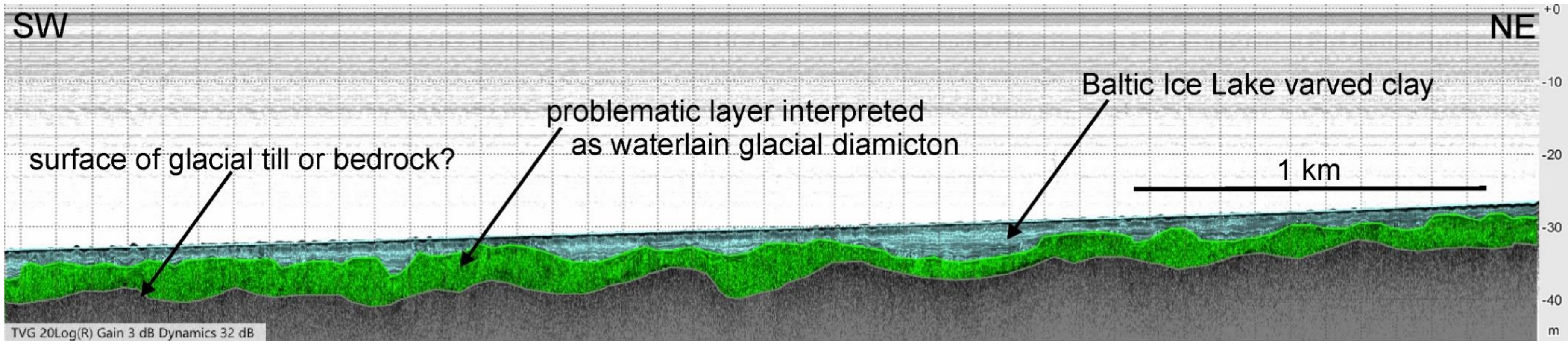

Fig. 35. Interpreted chirp-type seismo-acoustic profile from the central part of the WFA. For location of the profile, see line 11 in Fig. 21

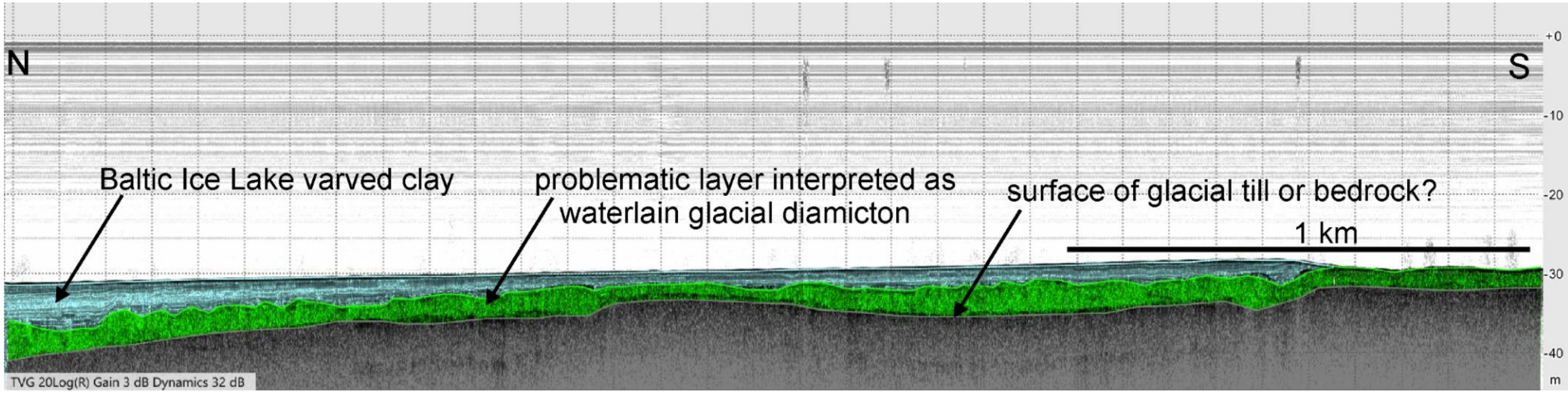

Fig. 36. Interpreted chirp-type seismo-acoustic profile from the central part of the WFA. For location of the profile, see line 12 in Fig. 21

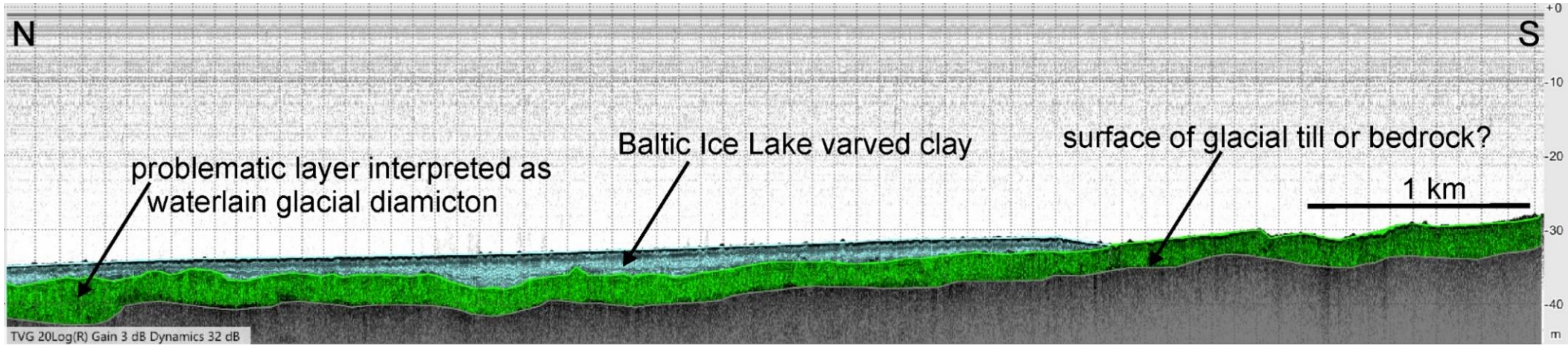

Fig. 37. Interpreted chirp-type seismo-acoustic profile from the central part of the WFA. For location of the profile, see line 13 in Fig. 21

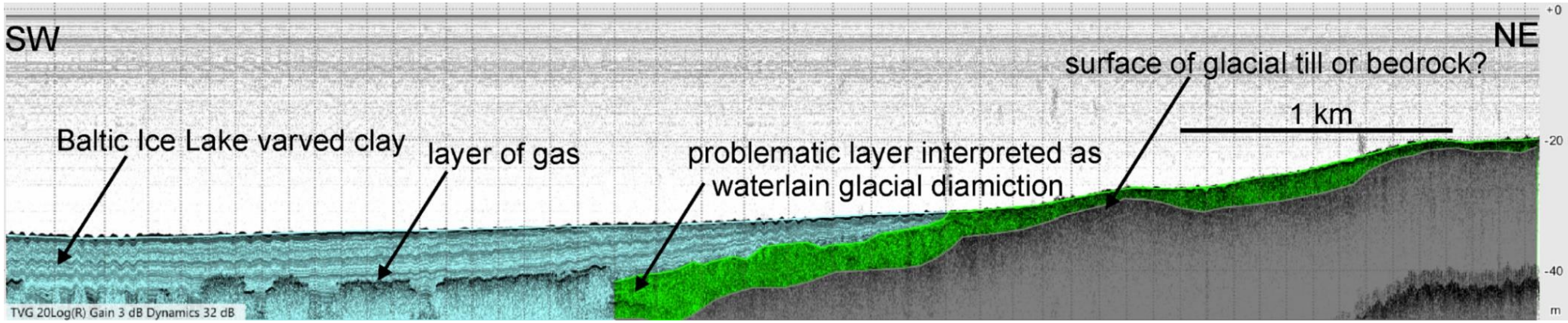

Fig. 38. Interpreted chirp-type seismo-acoustic profile from the southern part of the WFA. For location of the profile, see line 14 in Fig. 21

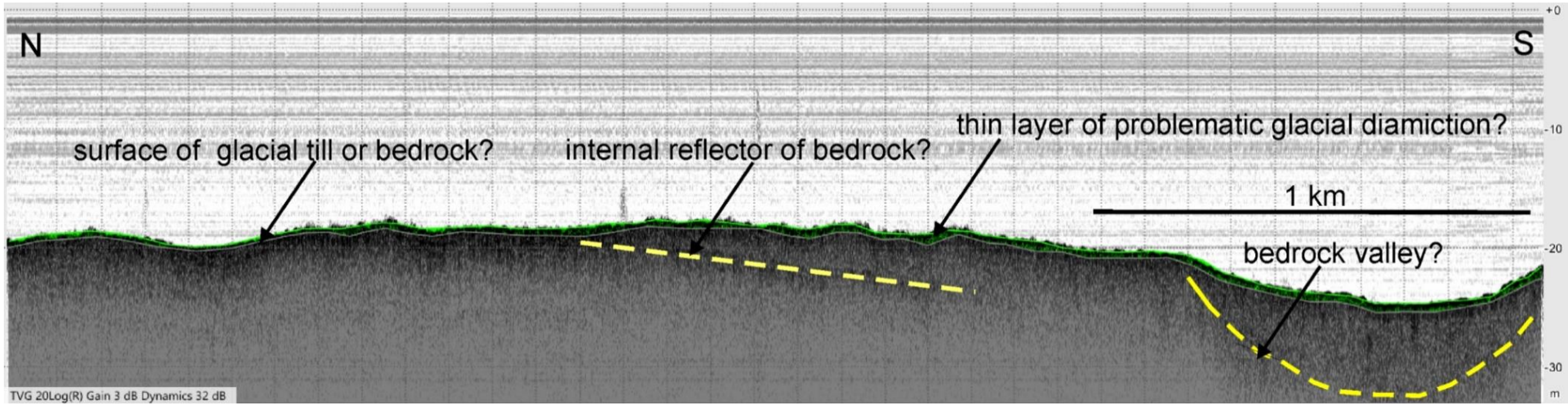

Fig. 39. Interpreted chirp-type seismo-acoustic profile covering the limestone plateau in the southern part of the WFA. For location of the profile, see profile 15 in Fig. 21

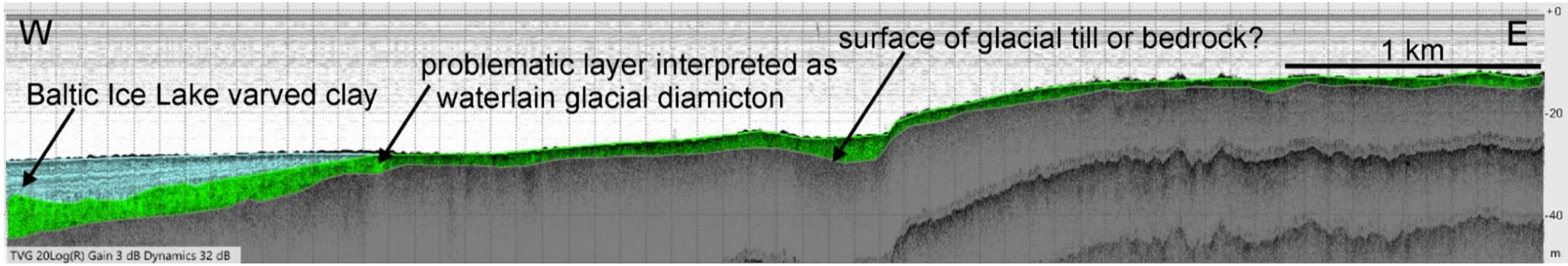

Fig. 40. Interpreted chirp-type seismo-acoustic profile from the southern part of the WFA. For location of the profile, see line 16 in Fig. 21

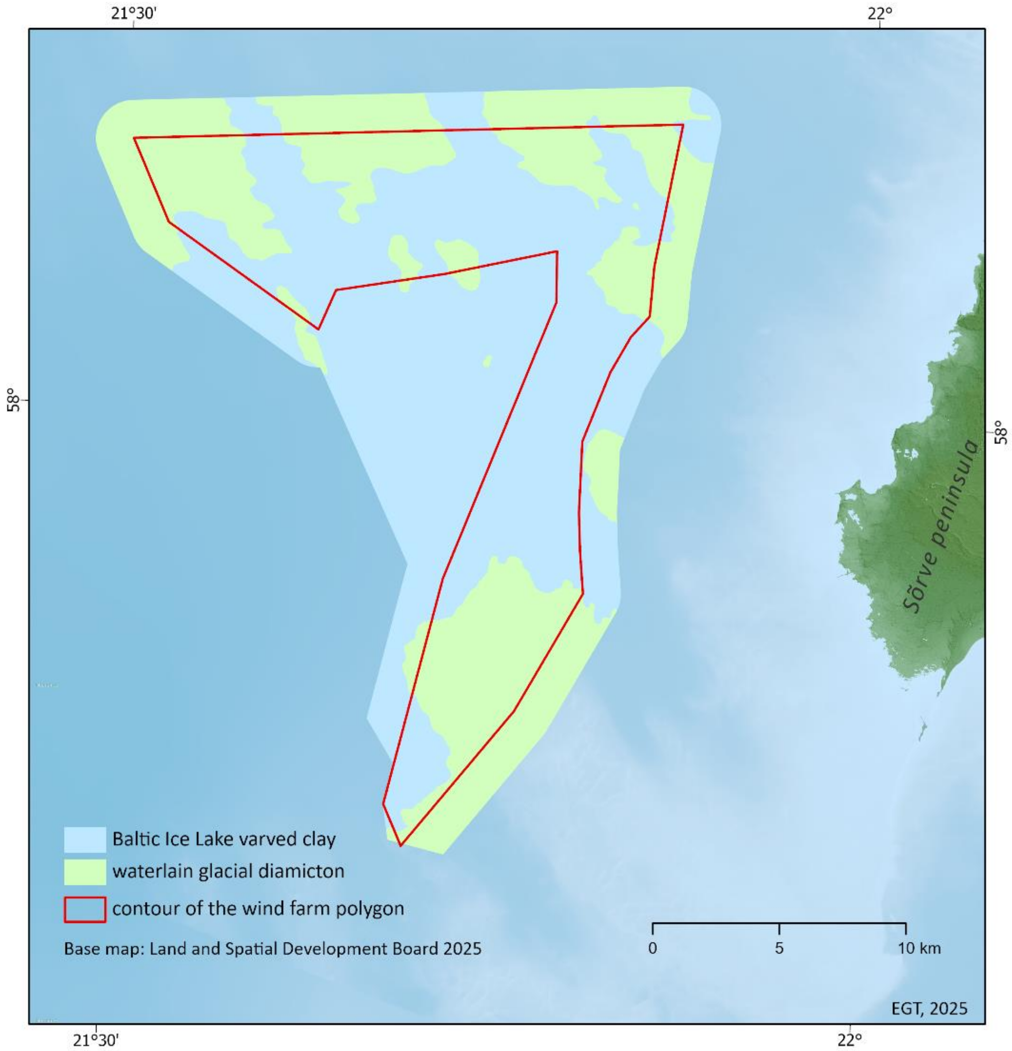

Fig. 41. Map of the Quaternary sediments around the WFA. The varved clay outcrop covers the low-lying areas of the bedrock depression. Elevated glacial till/bedrock surface surrounding the depression is everywhere covered by a (thin) problematic layer of waterlain glacial diamicton

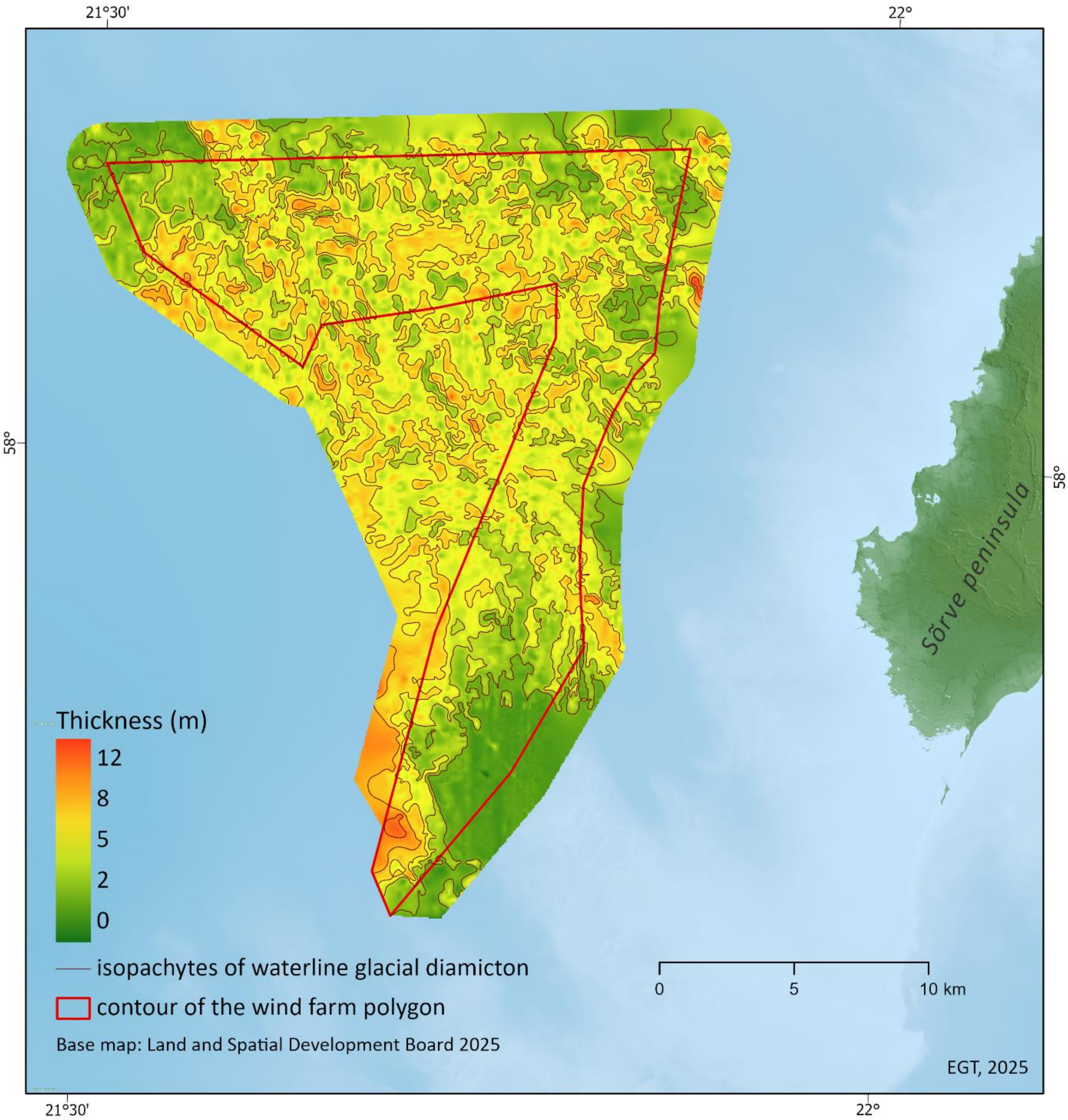

Fig. 42. Thickness map of the waterlain glacial diamicton around the WFA

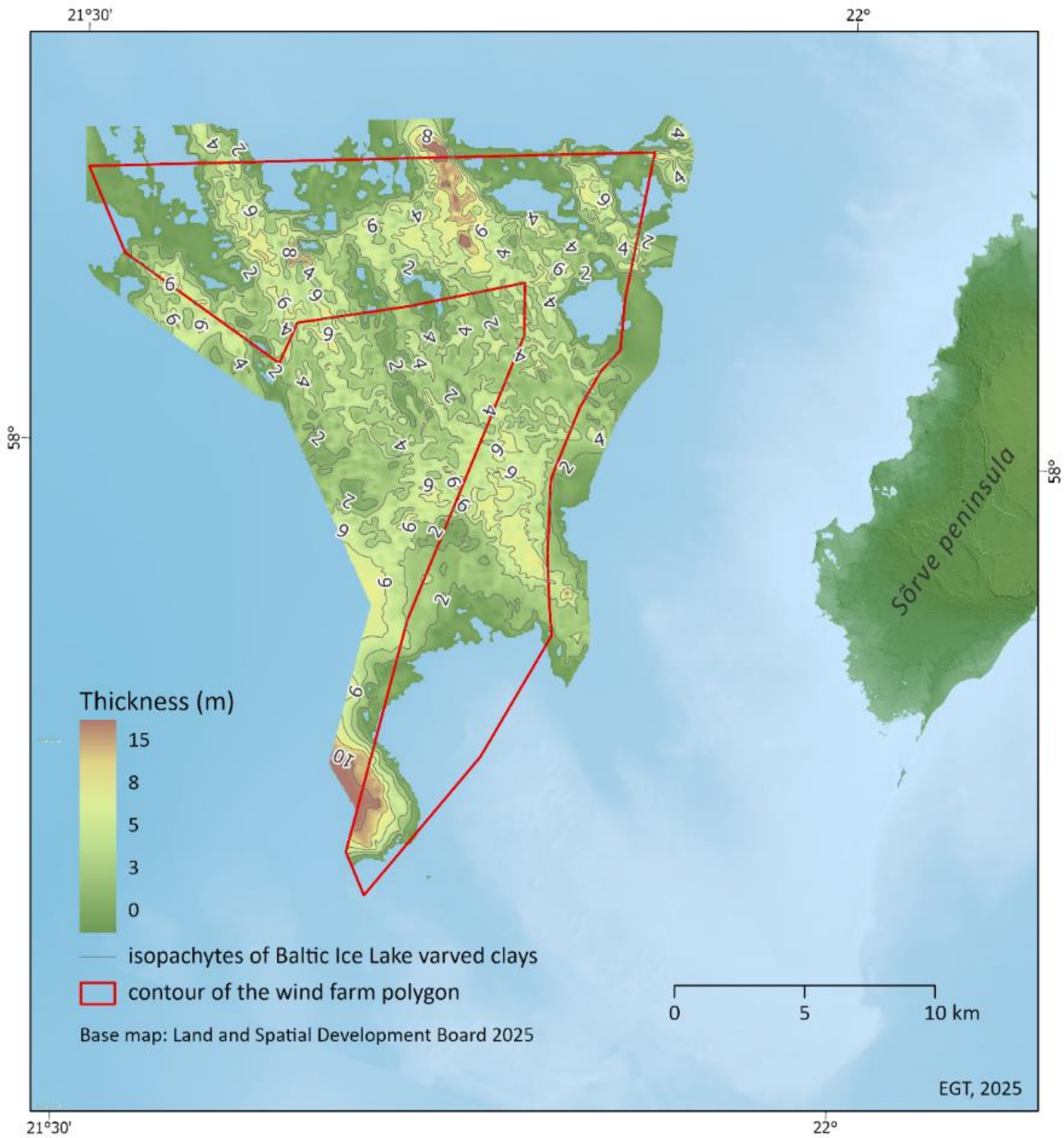

Fig. 43. Thickness and distribution map of the Baltic Ice Lake varved clay unit around the WFA

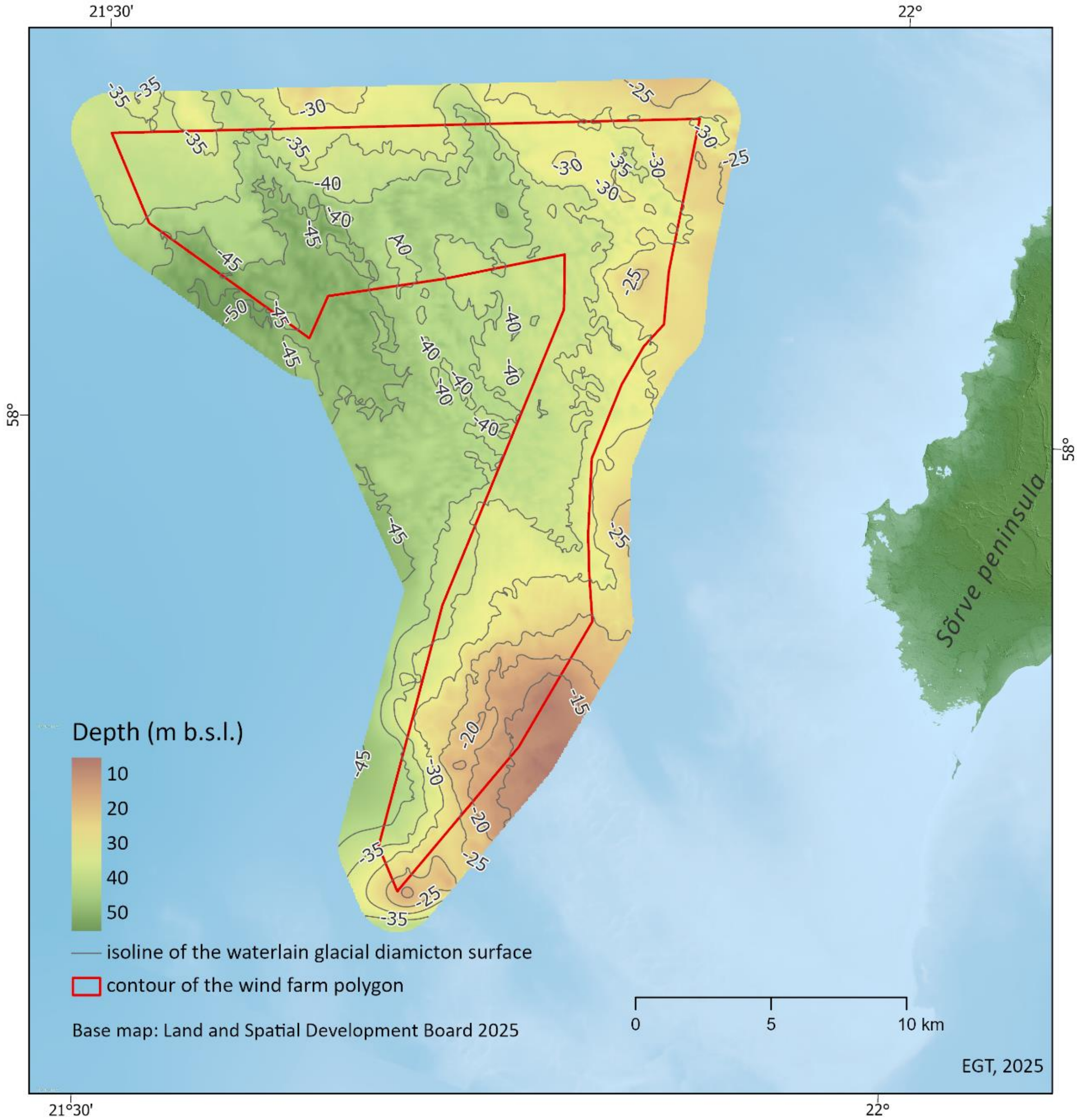

Fig. 44. The depth (relief) of the upper surface of the waterlain glacial diamicton around the WFA

1.6. Conclusions and suggestions for further studies of the geology of the offshore WFA to the west of the Sõrve peninsula

1. Geological information from the WFA is largely based on two sets of seismo-acoustic data. Airgun data collected in the early 1990s (allowing to follow the bedrock surface) and data recorded with a chirp-type seismo-acoustic transmitter in 2017–2024 (enables to study the postglacial Quaternary cover in detail).

2. The WFA is located on outcropping Silurian rocks that are largely represented by limestones with varying clay content of the Paadla, Kuressaare, Kaugatuma and Ohesaare stages around the WFA (Fig. 11).

3. The bedrock relief (depth) along the western coast of Saaremaa reveals two large entities: 1) the limestone plateau with outcropping hard, erosion-resistant limestones (the Jaani, Jaagarahu and-Rootsiküla stages) in the north (Fig. 11) that, 2) transfers to a bedrock slope and depression further to the south offshore the Sõrve peninsula, around the WFA.

4. The depth of the limestone plateau varies largely around 20–30 m b.s.l. (Figs 13 and 15) and within 40–60 m b.s.l. in the slope area where the WFA is largely located (Figs 13–20). However, some airgun profiles indicate that the bedrock surface may reach more than 80 m b.s.l. at the bottom of a solitary valley located near (likely outside) the southern margin of the E-W oriented segment of the wind farm polygon, (Figs 16 and 17).

5. Both the multibeam echo sounding and backscatter data show that the N and E margins of the 7-shaped wind farm polygon are partially located on the elevated bedrock (limestone plateau) area, where the thickness of the Quaternary sediments is insignificant, or they are possibly absent (Figs. 6–8 and 8A).

6. As the pulse of a chirp-type transmitter normally bounces entirely back from the glacial till surface, and thus allows to study only the postglacial till Quaternary sequence, distinguishing glacial till and bedrock surfaces in profiles where glacial till is missing is complicated (problematic). This is possibly the case around the WFA and reason why the seismo-acoustically impenetrable level in chirp-type recordings is interpreted as the glacial till/bedrock surface (Figs 26–-40).

7. Two distinctive postglacial Quaternary units emerge in the seismo-acoustic profiles generated by a chirp-type transmitter: 1) the problematic (likely clay-rich?) layer resting on the glacial till/bedrock surface that was interpreted as waterlain glacial diamicton is overlain, 2) by the Baltic Ice Lake varved clay unit (Figs 22 and 26–40).

8. Both these units make up also the map of the Quaternary sequence of the WFA off the Sõrve peninsula (Fig. 41). The waterlain glacial diamicton is exposed on the high elevated bedrock areas with an insignificant Quaternary cover, i.e. in the areas that emerge clearly also in the multibeam echo-sounder and backscatter maps (Figs 6–8 and 8A), as well as on the maps drawn along the bedrock/glacial till surface (Figs 23–25). The Baltic Ice Lake varved clay unit, however, was deposited and is exposed only in the low-lying bedrock areas, i.e. in the bedrock depression and incised into bedrock plateau valleys (Fig. 41).

9. The thickness of the waterlain glacial diamicton unit varies practically from zero in the areas of high elevated bedrock outcrops, up to 10 m in the low-lying bedrock depression (valleys). The Baltic Ice Lake varved clay unit that is absent from the elevated bedrock areas reaches in the bedrock depression slightly more than 10 m in thickness. Thus, the total thickness of the postglacial Quaternary sequence over the bedrock/glacial till surface in the WFA grows from zero to nearly up to 20 m in the southern corner of the wind farm polygon (Fig. 25).

10. The sea bottom around the WFA is widely covered by a layer of present sandy sediments, which is loose and thus easily shifted by waves and bottom currents. This is expressed by ripple marks that are seen in the multibeam echo sounder map, as well as in the chirp-type seismo-acoustic recordings (Figs 6, 22 and 28).

11. Significant number of boulders emerge on the elevated bedrock patches along the eastern margin of the NE-SW trending segment of the 7-shaped wind farm polygon. Especially on the shallowest bedrock elevation that intrudes into the southern part of this segment, where the sea depth decreases up to 12 m (Figs 6 and 7).

12. A special study around the WFA is needed, using simultaneous boomer- and chirp-type measurements, for contouring the bedrock surface and confirming the presence of the glacial till layer. A drill core is needed for specifying the genesis and composition of the problematic layer resting on the bedrock/glacial till surface, which was tentatively interpreted by us as waterlain glacial diamicton.

2. Overview of seismicity around the prospective wind farm area offshore the Sõrve peninsula, western Saaremaa

2.1. Introduction

The region of Estonia is only modestly seismically active due to its location at the northern edge of the east European sedimentary platform overlying the southeast flank of the stable Fennoscandian shield (e.g., Tuuling and Flodén, 2016). Seismic monitoring performed by the Geological Survey of Estonia (EGT) during the recent decades indicates that sporadic occurrence of minor (magnitude < 3) earthquakes within the country and its territorial waters is characteristic. As the potential wind farm area (WFA) is located at the southwestern corner of the region monitored by EGT, the area of seismic activity examined here extends to the west and south. Accordingly, an area of 56.5–59.5°N, 18–26°E was chosen for this study (Fig. 45). The principal reference for the presented earthquakes (Table 1) is the 2014 version of the FENCAT catalogue of earthquakes in Fennoscandia and Baltics, maintained by the Institute of Seismology, University of Helsinki (Ahjos & Uski, 1992; FENCAT, 2014). This catalogue is currently undergoing an update (Uski et al., 2025). As a result, magnitudes of a few earthquakes presented here will later be adjusted. Origins of some events are labelled in Table 1 as likely to be some other phenomena than tectonic movements (Korja et al., 2019). Earthquakes in Estonia located by EGT during 2015–2023 are also included in the list.

2.2. Earthquakes around the study area

It is somewhat challenging to achieve a comprehensive understanding of seismicity in areas of low activity. As return periods of earthquakes are long, centuries of observations would be needed. If notions regarding events back in history are taken into account, the level of inaccuracy increases inevitably. Locations and sizes of historical earthquakes can be assessed only macroseismically, i.e. basing on the impact of shaking and other related phenomena on people, buildings and landscape. Moreover, other events such as frost cracking, thunderstorms or meteotsunamis may have caused similar phenomena as tectonic earthquakes. Long data gaps may exist due to other reasons than real lack of seismicity. It is also likely that the level of historical seismicity is underestimated in sea areas far from inhabited land.

The first two entries in Table 1 are from the Gotland Island from 1374 and 1540, with magnitudes 4.0 and 4.3, respectively. They should be considered with reservations, particularly the earlier one. Also, the first known earthquake in mainland Estonia, a magnitude-3.9 event near Pärnu in February 1670 was more likely a frost-related event. Within Estonia, the first convincing notion of a real earthquake is of an event in the Haapsalu area in September 1827, when thundering sound was audible at several locations and vibration was felt at places (Doss, 1909).

Of particular interest for this study is the magnitude-2.6 historical earthquake on 18 May 1857 with the location at the Irbe Strait (Doss, 1909). Other epicentres relatively near the WFA belong to an earlier historical magnitude-3.5 event with less accurate details on 31 October 1785 and a location near the Latvian town Ventspils (Doss, 1909), an instrumentally recorded magnitude-2.3 earthquake to the north of the Latvian town of Kuldīga on 2 June 1982, and the magnitude-1.6 Kirbla earthquake in western Estonia on 28 January 2004. No later earthquakes have been detected at similar distances to the WFA as these events.

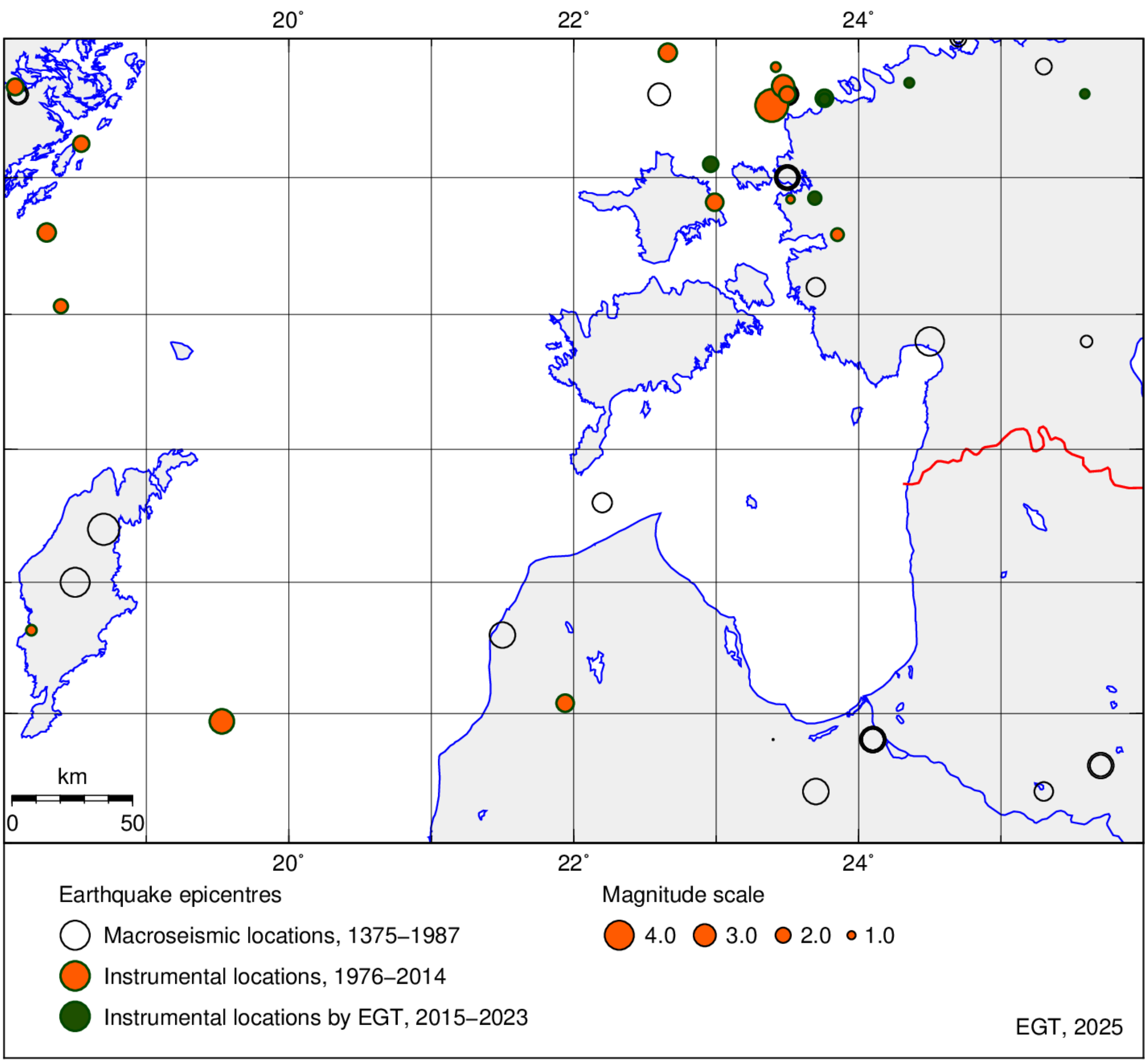

Fig. 45. Epicentral locations of the known earthquakes in the area surrounding the potential wind farm area during the period 1375–2023

Seismic stations measuring local earthquakes in northern Europe were gradually deployed during the latter half of the 20th century. Estonian earthquakes have been instrumentally measured from the beginning of the 21st century. A striking and unexpected exception is the magnitude-4.5 Osmussaar earthquake on 25 October 1976 (Table 1, Slunga 1979). This event is outstandingly large in these geological conditions and illustrates that noticeable earthquakes are not impossible in stable continental areas. However, they are expected to have long return periods, likely in the time span of several centuries.

Introduction of instrumental measurements, here during the few latest decades, provides a more detailed picture of seismicity. Events of smaller magnitudes are detected, and they have more reliable estimates of epicentres and depths. The apparent larger number of events is due to lowered detection threshold (currently approximately 1.5 in magnitude in this area).

Table 1. Catalogue of earthquakes in the area 56.5–59.5°N, 18–26°E

Date yyyymmdd	Time (UTC) hhmmss	°N	°E	Depth km	Magni- tude	Notes M – macroseismic, I - instrumental
1374	?	57.5	18.5	10	4.0	M, Questionable
1540	?	57.7	18.7	5	4.3	M
16700201	22	58.4	24.5	8	3.9	M, Possibly frost-related, not tectonic earthquake
178303	?	56.9	23.4	?	?	M
17851031	00	57.3	21.5	?	3.5	M
18070223	01	56.9	24.1	?	2.9	M
18210220	??	56.7	25.3	0	2.5	M
18270928	09	59.0	23.5	14	3.4	M
18440112	22	58.6	23.7	6	2.5	M, Possibly frost-related, not tectonic earthquake
18530121	0130	59.3	18.1	1	2.7	M, Possibly frost-related, not tectonic earthquake
18530204	2345	56.8	25.7	?	3.5	M
18530205	?	56.8	25.7	?	2.9	M
18530326	0130	59.5	24.7	5	1.2	M, Possibly not tectonic earthquake
18531229	?	56.9	24.1	?	3.5	M
18540105	?	56.9	24.1	?	2.9	M
18570518	09	57.8	22.2	1	2.6	M
18580115	1110	59.3	22.6	8	3.0	M, Possibly meteotsunami, not tectonic earthquake
18690215	00	59.5	24.7	6	2.1	M
18700206	0245	56.9	24.1	0	3.5	M
18700206	0320	56.9	24.1	0	2.9	M
18771016	0225	59.0	23.5	10	2.6	M, foreshock
18771016	0225	59.0	23.5	10	3.0	M, main shock
18960920	13	56.7	23.7	?	3.5	M
19041020	?	59.3	18.1	4	2.2	M
19090602	0830	58.4	25.6	7	1.5	M

Date yyyymmdd	Time (UTC) hhmmss	°N	°E	Depth km	Magni-tude	Notes M – macroseismic, I - instrumental
19310712	22	59.4	25.3	5	2.1	M
19761025	083945	59.26	23.39	10	4.5	I, felt, main shock
19761025	0849	59.3	23.5	?	3.0	M, aftershock
19761025	0907	59.3	23.5	?	2.6	M, aftershock
19761108	101707	59.33	23.47	?	3.0	I, felt, aftershock
19761122	121442	59.3	23.5	13	2.1	I, felt, aftershock
19800109	012452	58.91	22.99	?	2.3	I
19800524	030252	58.8	18.3	?	2.4	I
19810426	000453	58.53	18.40	7	1.8	I
19810622	192737	59.45	22.66	7	2.4	I
19820602	075817	57.04	21.94	?	2.3	I
19870408	1921	58.4	26.1	7	3.0	M
19880429	153652	56.97	19.53	1	3.3	I
20030112	114347	59.398	23.419	10	1.2	I
20040128	154000	58.792	23.851	10	1.6	I, felt
20050927	035539	57.318	18.193	2	1.3	I
20060524	232722	59.327	18.079	0	2.2	I
20130204	201754	58.921	23.522	4	1.0	I, felt
20140708	021651	59.122	18.543	11	2.1	I
20170322	030027	59.342	24.356	4	1.2	I
20170715	080150	59.048	22.961	11.4	2.0	I
20180304	012144	58.925	23.692	3.5	1.7	I, felt
20220613	031053	59.286	23.760	4.0	2.3	I, felt, main shock
20220628	173454	59.283	23.761	4.0	1.4	I, felt, aftershock
20220903	023612	59.302	25.588	2.4	1.1	I

2.3. Estimation of seismic hazard in the study area

Seismic hazard is a natural phenomenon generated by an earthquake (e.g., ground shaking, fault rupture, soil liquefaction) and seismic risk is an interaction between seismic hazard and vulnerability of people or built environment (e.g., Wang 2009). Seismic hazard has been evaluated for Europe by collecting data from relevant institutions around the whole continent. A recent version of the hazard map has been issued (see Fig. 46 from Danciu et al., 2024). For the Fennoscandian region in this map, the 2014 version of the FENCAT catalogue was used (Uski et al., 2025).

Seismic hazard is expressed as peak ground acceleration (PGA) equal to the maximum ground acceleration occurring during earthquake shaking at a location. PGA can be expressed in fractions of g (standard acceleration due to Earth's gravity, equivalent to g-force, 1 g = 9.81 m/s^2). Fig. 46 presents mean PGA for a return period of 475 years, illustrating that seismic hazard is modest in the current study area reaching values of up to approximately 0.02–0.03 g.

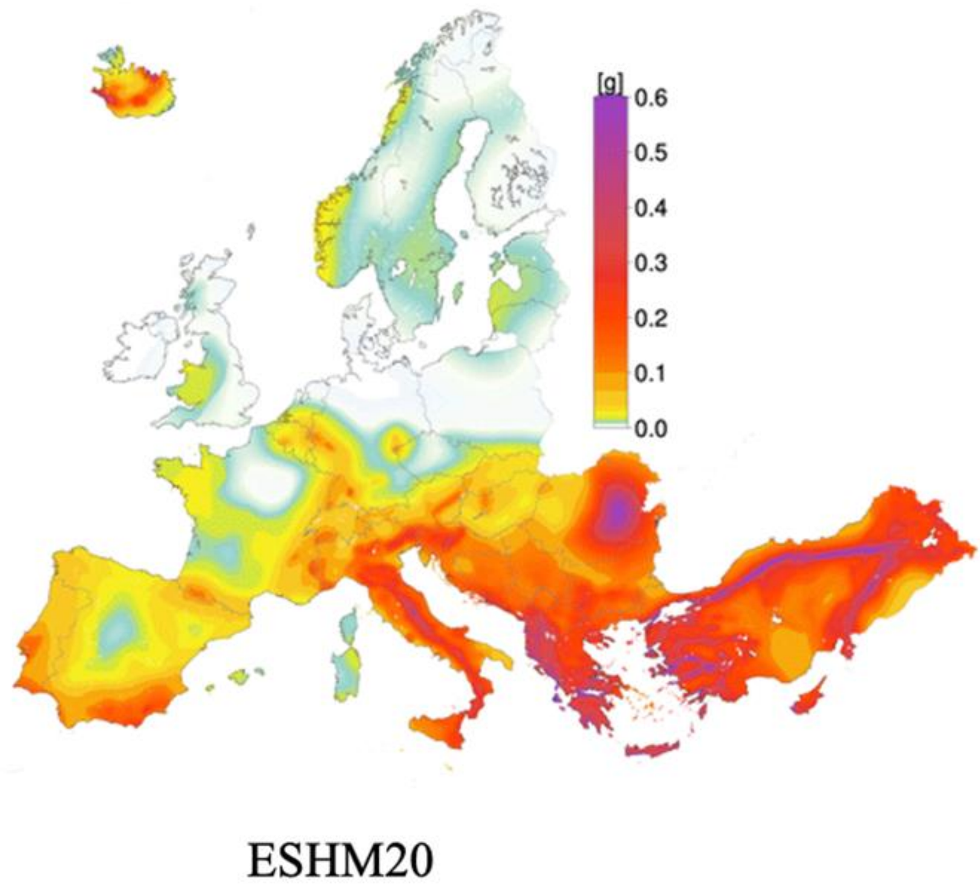

Fig. 46. Map of the European Seismic Hazard Model 2020, showing the mean peak ground acceleration for a return period of 475 years (from Danciu et al., 2024)

2.4. Conclusions regarding seismicity in the region surrounding the offshore WFA to the west of the Sõrve peninsula

Existing observations indicate that seismic activity is modest in the immediate vicinity of the WFA to the west of the Sõrve peninsula and in the region surrounding it. This is characteristic for an area with an old stable crystalline basement. Historical accounts date back several centuries, but earlier notions should be considered with reservations. Although there is the possibility that some other natural phenomena have been mistakenly interpreted as historical earthquakes, genuine earthquakes have certainly taken place. It can be presumed that there are long data gaps, particularly for offshore areas. Data have become more reliable towards the 19th century and quite precise instrumental observations exist for the recent decades. A rough estimate for the detection threshold of earthquakes in this region is magnitude 1.5.

Although far-fetched conclusions cannot be made due to sparsity of data, it can be stated that the study area experiences modest seismicity. Accordingly, also the seismic hazard can be regarded to be modest.

Kokkuvõte

Käesolevas aruandes käsitletakse Saaremaa läänerannikule, Sõrve poolsaarest ~10–40 km läände planeeritava perspektiivse, 7-kujulise avamere tuulepargi ala (polügooni) geoloogilist ehitust ja hinnatakse selle seismilisuse tausta. Ala geoloogilise ehituse kirjeldus tugineb suuresti kahele seismo-akustilise andmestiku kogumile: 1) 1990 aastate alguses Rootsi-Eesti koostöös madalsagedusliku (250–500 Hz) suruõhu kahuri abil kogutud profileerimise andmestik, mis annab ettekujutuse tuulepargi alla jääva ala aluspõhja sügavusest ja reljeefist, 2) aastatel 2017–2024 Eesti Transpordi (Veeteede) Ameti poolt selles piirkonnas lehviksonari ja *chirp*-tüüpi saatja (2–9 kHz) abil läbi viidud merepõhja kaardistamise andmestikule, mis aitab detailiseerida merepõhja reljeefi ja aluspõhjal lasuva pinnakatte läbilõiget.

Meresügavus, mis üldjoontes suureneb Sõrve säärest Läänemere keskosa suunas, varieerub tuulepargi alal vahemikus 12 m selle rannalähedases lõunaosas kuni ligi 45 m rannikust eemale jäävas läänesopis. Merepõhja sügavusjoon(ed) 30 ja 35 m eristavad nii põhjareljeefi iseloomu kui ka geoloogilist ehitust silmas pidades kaht selgelt erinevat piirkonda. Esimesest sügavusjoonest ida ja teisest põhjasuunas jääb liigestatud põhjareljeefiga, õhukese (kohati olematu) pinnakattega madalveelisem lubjakivi platoo. Nimetatud sügavusjoontest läände ja edelasse jääb kergesti erodeeritavatesse Kuressaare, Kaugatuma ja Ohesaare lademe savikatesse lubjakividesse erodeeritud aluspõhja nõgu. Erinevalt madalveelisest, sisuliselt olematu pinnakattega lubjakivi platoost, kus tõenäoliselt kohati paljandub ka aluspõhi (õhukese moreeni või savimoreeniga kaetud aluspõhi), on aluspõhja nõgu ja selle nõlvaala mattunud pärast jääaja sette kompleksi alla. Seetõttu on merepõhi tuulepargi ala selle sügavamas avamere poolses osas tasane. Aluspõhja sügavus tuulepargi lubjakivi platoo ning nõlva-nõo aladel jääb suuresti vastavalt 25–35 m ja 40–60 m alla poole merepinda, aga võib üksikus suruõhu kahuri profiilil esile tulevas orundis ületada isegi 80 m.

Kuna *chirp*-tüüpi saatja seismo-akustiline impulss peegeldub enamasti täielikult tagasi pea et kõikjal Eestis aluspõhja katvalt moreenikihi pinnalt, siis moreenikihi puudumisel ei võimalda see meetod ühemõtteliselt tuvastada, kas seismilisele impulsile läbimatu pind markeerib moreenikihi või aluspõhja pealispinda. Selline juhtum esineb ilmselt tuulepargi alal, mis ei võimalda lisaks moreeni kihile fikseerida ühemõtteliselt ka selle ülemist pinda, mistõttu seismo-akustiliselt läbimatut taset käsitletakse aruandes aluspõhja-moreeni pealispinnana. Sellel pinnal lasuv Kvaternaari kompleks jaguneb selgelt kaheks, seismo-akustilise signatuuri järgi ilmselt savirikkaks üksuseks, mis mõlemad on tõenäoliselt ladestunud liustikujärve tingimustes. Aluspõhja-moreeni pinnal lasub ilmselt savimoreen (savirikas, üksikuid kivi ja kruusatükk sisaldav kiht) ja sellel omakorda Balti jääjärve viirsavide kompleks. Aluspõhja-moreeni pinda kattev savimoreen levib sisuliselt kõikjal tuulepargi ala piires, kuigi selle paksus aluspõhja platoo piires, kus see kiht avaneb, võib kohati kahaneda nullini. Tuulepargi alla jääva aluspõhja nõo ning selle nõlva piires, kõigub savimoreeni paksus suuresti 4–6 m piires, ulatudes tuulepargi ala lõunatipu ümber ligi 10 m. Balti jääjärve viirsavid tuulepargi alal on ladestunud üksnes aluspõhja nõos ja selle nõlval, kus see kiht, mille paksus kõigub 2–6 m piires, avaneb kõikjal ka mere põhjas. Selleks et kontuurida tuulepargi alal moreenikihi levikut ning fikseerida ühemõtteliselt selle ülemine pind tuleb see piirkond katta seismo-akustiliste profiilide võrguga, kus lisaks *chirp*-tüüpi saatjale kasutatakse samaaegselt ka *boomer*-tüüpi saatjat, mille impulss läbib enamasti moreenikihi.

Tuginedes seismo-akustilistel profiilidel ja lehviksonari kaardil esile tulevatele virgmärgi laadsetele struktuuridele, ilmneb, et viirsavide avamusalal on merepõhi laialdasel alal mattunud tänapäevaste liivakate setetega, mis on hoovuste ja lainetuse poolt kergesti liigutatavad. Lehviksonari kaardi tulevad tuulepargi idapiiril esinevatel lubjakivi platoo laikudel merepõhjas esile arvukad, suuremad ja väiksemad rändrahnud.

Kuna Eesti piirkond asub geoloogiliselt stabiilsel alal, on ka seismilisuse tase tagasihoidlik. Viimaste aastakümnete instrumentaalsete mõõtmiste baasil on ootuspärane, et aeg-ajalt toimuvad erinevates asukohtades tagasihoidliku magnituudiga (< 3) maavärinad. Tuulepargi jaoks vaadeldi ala selle ümber, mis ulatub ka Eestist läände ja lõuna, piiridega 56,5–59,5°N, 18–26°E. Põhiliseks andmestikuks oli 2014. aasta versioon kataloogist FENCAT, mis hõlmab Põhjamaade ja Baltikumi seismilisust ja mida haldab Helsingi Ülikooli Seismoloogia Instituut. Lisatud on ka Eesti Geoloogiateenistuse poolt Eestis lokaliseeritud maavärinad ajavahemikus 2015–2023.

Tagasihoidliku seismilisuse piirkondade osas on väljakutseks, et on raske kätte saada tervikpilti aktiivsusest. Selleks oleks vaja vaatluseid sajandite vältel, aga kahjuks on ajaloolised andmed ebatäpsed ja lünklikud. Alles viimastel aastakümnetel on hakatud rajama seismojaamu, mis võimaldavad täpsemat lokaliseerimist ning suudavad registreerida ka väiksemaid sündmuseid (antud piirkonnas tinglikult kuni magnituudini 1,5).

Silmatorkav sündmus uuringuala raames on magnituudiga 4,5 maavärin Osmussaare lähedal 25.10.1976. See näitlikustab, et ka geoloogiliselt rahulikes piirkondades pole võrdlemisi suured maavärinad välistatud. Siiski on seda laadi sündmuseid oodata harva, eeldatavasti kord mitme sajandi vältel.

Olemasoleva maavärinate nimekirja ning hiljuti publitseeritud Euroopa seismilise ohu kaardi (European Seismic Hazard Map 2020) baasil saab tõdeda, et eeldatav seismilise ohu tase on piirkonnas pigem madal, kuigi andmete vähesuse tõttu pole võimalik teha kaugele minevaid järeldusi.

References

Ahjos, T. & Uski, M., 1992. Earthquakes in northern Europe in 1375–1989. Tectonophysics, 207(1–2), 1–23. https://doi.org/10.1016/0040-1951(92)90469-M

Danciu, L., Giardini, D., Weatherill, G., Basili, R., Nandan, S., Rovida, A., Beauval, C., Bard, P.-Y., Pagani, M., Reyes, C. G., Sesetyan, K., Vilanova, S., Cotton, F. & Wiemer, S., 2024. The 2020 European Seismic Hazard Model: overview and results. NHESS, 24(9), 3049–3073. https://doi.org/10.5194/nhess-24-3049-2024

Doss, B., 1909. Die historisch beglaubigten Einsturzbeben und seismisch-akustischen Phänomene der russischen Ostseeprovinzen. Beiträge zur Geophysik X, 1–124 (in German).

FENCAT, 2014. The 2014 release of the Fennoscandian earthquake catalogue FENCAT. Institute of Seismology, University of Helsinki. https://www.seismo.helsinki.fi/bulletin/list/catalog/Scandia_2014.html

Kaljo, D., (ed.), 1970. The Silurian of Estonia. Valgus, Tallinn, 343 pp. (in Russian with English summary).

Kaljo D., (ed.), 1977. Facies and fauna of the Baltic Silurian. Tallinn, 286 pp. (in Russian with English summary).

Karpin, V., Heinsalu, A. & Virtasalo, J. J., 2021. Late Pleistocene iceberg scouring in the north-eastern Baltic Sea, west of Estonia. Marine Geology, 438, 106537. https://doi.org/10.1016/j.margeo.2021.106537

Korja, A., Kihlman, S. & Oinonen, K. (eds), 2019. Seismic source areas for seismic hazard assessment in Central Fennoscandia. Institute of Seismology, University of Helsinki, Report S-66, 228 pp.

Lutt, J. & Raukas, A. (eds), 1993. Geology of the Estonian shelf. Estonian Geological Society, Tallinn, 178 pp. (in Estonian with English summary).

Nestor, H., 1997. Silurian. In: Raukas, A. & Teedumäe, A. (eds), Geology and Mineral Resources of Estonia. Estonian Academy Publishers, Tallinn, pp. 89–105.

Raukas, A., 1978. Pleistocene deposits of the Estonian SSR. Valgus, Tallinn, 310 pp. (in Russian with English summary).

Raukas, A. & Teedumäe, A., (eds), 1997. Geology and mineral resources of Estonia. Estonian Academy Publisers, Tallinn, 436 pp.

Tavast, E. & Raukas, A., 1982. The bedrock relief of Estonia. Valgus, Tallinn, 192 pp. (in Russian with English summary).

Tsyrulnikov, A., Tuuling, I., Kalm, V., Hang, T. & Flodén, T., 2012. Late Weichselian and Holocene seismo-stratigraphy and depositional history of the Gulf of Riga, NE Baltic Sea. Boreas, 41(4), 673–689.

Tuuling, I. & Flodén, T., 2009. The Llandovery - lowermost Wenlock sequence in the Baltic Sea between Saaremaa and Gotland; subdivision, thicknesses and correlation, based on marine seismic studies. Marine Geology, 267(1–2), 55–70.

Tuuling, I. & Flodén, T., 2011. Seismic stratigraphy, architecture and outcrop pattern of the Wenlock-Přidoli sequence offshore Saaremaa, Baltic Sea. Marine Geology, 281(1–4), 14–26.

Tuuling, I. & Flodén, T., 2013. Silurian reefs offshore Saaremaa and their extension towards Gotland, central Baltic Sea. Geological Magazine, 150, 923–936.

Tuuling, I. & Flodén, T., 2016. The Baltic Klint beneath the central Baltic Sea and its comparison with the north Estonian Klint. Geomorphology 263, 1–18. https://doi.org/10.1016/j.geomorph.2016.03.030

Tuuling, I., Suuroja, S. & Ausmeel, M., 2022. The outlines of the bedrock relief and the Quaternary cover between the Estonian mainland and the islands of Muhu and Saaremaa in the West Estonian Archipelago. Estonian Journal of Earth Sciences, 71(2), 111–126. https://doi.org/10.3176/earth.2022.08

Uski, M., Oinonen, K., Lund, B., Soosalu, H., Ottemöller, L., Sørensen, M. B., Voss, P. & Korja, A., 2025. Submitted to Geophysical Journal International.

Wang, Z., 2009. Seismic Hazard vs. Seismic Risk. Seismol. Res. Lett., 80, 673–674.

Appendix 1

List of datafiles (.shp):

- ✓ Seismo-acoustic (Chirp) profiles
- ✓ Isolines of glacial till/bedrock surface
- ✓ Isopachytes of postglacial sediments
- ✓ Isopachytes of waterlain glacial diamicton
- ✓ Isopachytes of Baltic Ice Lake varved clays
- ✓ Isolines of walterlain glacial diamicton surface
- ✓ Quaternary sediments around the wind farm polygon

File sets of ESRI grid (raster) files:

Relief of glacial till/bedrock surface

Thickness of postglacial sediments

Thickness of the waterlain glacial diamicton

Thickness of the Baltic Ice Lake varved clays

Relief of the surface of waterlain glacial diamicton

Backscatter files:

elwind_backscatter_a0.TIFF

Bathymetry files:

elwind_bathymetry_clipped.TIF